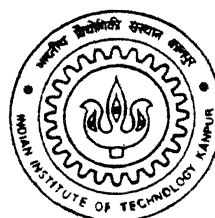


97/06/17

# STUDY OF THE CERAMIC/METAL INTERFACE STRUCTURE

By  
SYED BADIRUJJAMAN

MME  
1999  
B1428



DEPARTMENT OF MATERIALS AND METALLURGICAL ENGINEERING  
**INDIAN INSTITUTE OF TECHNOLOGY, KANPUR**

DECEMBER, 1998

# STUDY OF THE CERAMIC/METAL INTERFACE STRUCTURE

*A Thesis Submitted*  
in Partial Fulfillment of the Requirements  
for the Degree of  
Master of Technology

by  
**SYED BADIRUJJAMAN**



to the  
MATERIALS AND METALLURGICAL ENGINEERING  
INDIAN INSTITUTE OF TECHNOLOGY KANPUR  
DECEMBER 1998

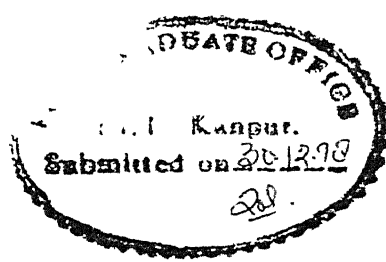
26 MAR 1999

CENTRAL LIBRARY  
I.I.C., KANTUR

No. A 127794



A127794



## CERTIFICATE

It is certified that the work contained in this thesis entitled "*Study of the ceramic/metal interface structure*", by *Syed Badirujjaman*, has been carried out under my supervision and that this work has not been submitted elsewhere for any degree.



Dr. S.P.GUPTA

Professor

Materials and Metallurgical Engineering,  
Indian Institute of Technology, Kanpur

December, 1998

Dedicated to .....

My Grandmother

# Acknowledgement

I thank my guide, Prof. S. P. Gupta, for his guidance, inspiration and encouragement during the course of this project. He has taught me the values of research and independent thinking. He spent tremendous time and effort on me and was always ready to help and discuss my difficulties. It was a great pleasure working with him.

I must take the opportunity to thank my friends Somnath, Amrita, Sarbajit, Rajiv and Milan for their kind help in completing this thesis. I also would like to thank all the laboratory staffs who have helped me a lot, without which this thesis could not have been a reality. Finally I must thank my lab-mates Karthikeyan and Diwakar for their kind support to successfully complete this work.

# Abstract

The increasing technological interest of ceramic to ceramic and ceramic to metal joints in industrial and developmental application is due to the unique combination of properties of ceramic materials, namely high temperature strength, excellent wear resistance, high hardness, excellent corrosion and oxidation resistance, low thermal expansion, high electrical resistivity. Simultaneously as the catalog of materials expanded, the technology of metal to nonmetal joining method improved, and one of them, brazing has been an important method of joining. It has been used in the electrical, chemical and aeronautical industries for the manufacture of product required.

Whatever may be the application, a series of intermetallic layers form as a result of chemical reaction at different interfaces. For a simple metal-metal or metal-ceramic or ceramic-ceramic system a number of intermetallic compounds form, depending on the wettability of filler metal, presence of the active metal in the filler metal, and the characteristics of the ceramic used. Thermodynamics and kinetics decides their formation and growth behavior. Depending upon the compositions of the filler alloys and the base materials, a wide range of intermetallic layer may form in the ceramic/metal interface.

We have studied the formation and growth of intermetallic compounds in the ceramic to metal systems, which are produced by active brazing process. In this process alumina( $Al_2O_3$ ) was used as ceramic members, and 18-8 stainless steel, pure niobium(Nb) and pure iron(Fe) were used as the metal members, and Ag-28at%Cu and Ag-27at%Cu-10at%In alloys were used as the filler metals, and pure titanium(Ti) was used as the active metal. The brazing

process was carried out at 900°C and 800°C for different holding times under vacuum and cooled in air.

It was observed that Ag-27Cu-10In ternary filler alloy was more effective, with respect to compactness of the joint of ceramic to metal, than the Ag-28Cu filler alloy. It was also observed that Ti reacts with the ceramic surface as well as with the filler metal at high temperatures and forms different intermetallic layers. occurrence of some phases depends on the diffusion path. Some of the phases form through chemical reactions. At the Ti/filler metal interface,  $TiCu$ ,  $Ti_2Cu$ ,  $Ti_3Cu_4$ ,  $Ti_2Cu_3$  and  $TiCu_4$  phases from the Ti-Cu system, and  $TiFe$  and  $TiFe_2$  phases from the Ti-Fe system, and  $TiAg$  phase from the Ti-Ag system, formed in the diffusion couple. In the case of Ti/( $Al_2O_3$ ) interface,  $Ti_3Al$  and  $TiAl_3$  phases formed through chemical reactions. Part of the eutectic filler alloys, (Ag-28Cu) and (Ag-27Cu-10In) remain unreacted, with Ag-rich( $\alpha$ ) and Cu-rich( $\beta$ ) phases showing a eutectic structure next to the metal/filler metal interface. Some unknown ternary intermetallic compounds as well as binary compounds were also observed in the diffusion couple .

# Contents

List of Figures	ix
List of Tables	xi
1 Introduction	1
2 Literature Review	5
2.1 Key Parameters Of Brazing . . . . .	5
2.1.1 Surface Energy and Surface Tension . . . . .	5
2.1.2 Wetting and Contact Angle . . . . .	6
2.1.3 Fluid Flow and Factors Affecting the Fluid Flow . . . . .	8
2.1.4 Surface Roughness of Components . . . . .	9
2.1.5 Dissolution of Parent Materials by Molten Filler Metal . . . . .	9
2.2 Prime elements of the brazing process . . . . .	10
2.2.1 Temperature and time . . . . .	10
2.2.2 Surface Preparation . . . . .	11
2.2.3 Joint Design and Clearance . . . . .	12
2.2.4 Source and Rate of heating . . . . .	13
2.2.5 Joining atmosphere . . . . .	13
2.2.6 Filler metal flow and their characteristics . . . . .	14
2.3 Application of Phase diagram of Filler metals to Brazing . . . . .	15
2.3.1 Filler metals from binary alloy systems . . . . .	16
2.3.2 Filler metal from Ternary alloy system . . . . .	19
2.3.3 Reactive filler alloys . . . . .	23
2.4 Wetting of ceramic materials . . . . .	24
2.4.1 Wetting and Interface reaction of Alumina( $Al_2O_3$ ) . . . . .	24
2.4.2 Reactive wetting and Interfacial reaction of SiC by Active filler metal	26
3 Experimental Procedure	29
4 Results and Discussion	33
4.1 $Al_2O_3/Ti/Ag-28Cu/Pure Iron(Fe)$ System . . . . .	33

---

4.1.1	Phases from binary systems . . . . .	33
4.1.2	Phases from Ternary systems . . . . .	36
4.2	$Al_2O_3/Ti/Ag-28Cu/Stainless Steel(Fe-Ni-Cr)$ System . . . . .	38
4.2.1	Phases from Binary systems . . . . .	40
4.2.2	Phases from Ternary systems . . . . .	41
4.3	$Al_2O_3/Ti/Ag-28Cu/Pure Niobium(Nb)$ system . . . . .	42
4.3.1	Phases from Binary systems . . . . .	43
4.3.2	Phases from Ternary systems . . . . .	44
4.4	$Al_2O_3/Ti/Ag-27Cu-10In/Pure Iron(Fe)$ system . . . . .	45
4.4.1	Phases from Binary systems . . . . .	45
4.4.2	Phases from Ternary systems . . . . .	47
4.5	$Al_2O_3/Ti/Ag-27Cu-10In/Pure Niobium(Nb)$ system . . . . .	47
4.5.1	Phases from Binary systems . . . . .	48
4.5.2	Phases from Ternary systems . . . . .	49
4.6	$Al_2O_3/Ti/Ag-27Cu-10In/Stainless Steel(Fe-Cr-Ni)$ system . . . . .	51
4.6.1	Phases from Binary systems . . . . .	53
4.6.2	Phases from Ternary systems . . . . .	54
5	Conclusion	59
	References	61

# List of Figures

2.1	Simplified diagram of surface energies. . . . .	6
2.2	Surface tension forces acting when a liquid droplet wets a solid surface, according to the classical model. [2] . . . . .	7
2.3	Au-Ni phase diagram. The erosion of a Ni substrate by a Au-Ni braze and the associated change to the composition of the filler metal are indicated.[2] . . . . .	17
2.4	Ag-Cu phase diagram. Brazing of copper components with Ag-28Cu eutectic braze results in dissolution of copper into the molten filler metal. [2] . . . . .	18
2.5	Liquidus surface of the Ag-Au-Cu ternary system. [2] . . . . .	20
2.6	Isothermal projection of the Ag-Au-Cu phase diagram at 700°C A hypothetical tie line is shown linking the compositions of the two conjugate phases formed by the Ag-28Cu braze with a thin gold metallization. [2] . . . . .	21
2.7	Schematic section through the Ag-Au-Cu ternary system at 2% Au. [2] . . . . .	22
2.8	Isothermal section of the Ti-Al-O system at 1100°C and the diffusion paths between Ti and $Al_2O_3$ in finite(thin) and infinite(thick) couples. [5] . . . . .	26
3.1	Section of the assembly in which the specimen were prepared. . . . .	30
3.2	The line along which the brazed specimen was cut to expose the interface . . . . .	31
4.1	All the interfaces and layers of intermetallic compounds in the joint area of the specimen . . . . .	35
4.2	Different morphology of TiFc compound as a dark wavy layer at the Fe/filler metal interface . . . . .	36
4.3	$Ti_2Cu$ intermetallic compound forms as a polyhedral structure at the Ti/filler metal interface . . . . .	37
4.4	Different morphology of Ag-rich( $\alpha$ ) and Cu-rich( $\beta$ ) solid solution . . . . .	38
4.5	All the interfaces and layers of intermetallic compound at the joint area. . . . .	40
4.6	Morphology of TiCu and $Ti_2Cu$ intermetallic compound at the Ti/filler metal interface. . . . .	41
4.7	Eutectic structure of solid solution. . . . .	42
4.8	TiCu intermetallic compounds into the Ag matrix as a dark particle. . . . .	44
4.9	Unknown phase from Ag-Nb system as a spheroidal particle. . . . .	45
4.10	Rod-like nature of Cu-rich $\beta$ phase in the Ag matrix( $\alpha$ ). . . . .	46

4.11	All the interfaces and layers of intermetallic compounds formed into the joint area of the specimen. . . . .	48
4.12	Structure of $TiFe_2$ phase as a dark continuous layer next to the pure iron. . . . .	49
4.13	TiFe phase as a small dark layer at the Ti/filler metal interface. . . . .	50
4.14	All the interfaces and layers of intermetallic compounds into the joint area. . . . .	53
4.15	Layer of TiCu compound at the Nb/filler metal interface and the particle of $Ti_3Cu_4$ compound at the light matrix of Ag are shown. . . . .	54
4.16	Layer of $Ti_2Cu$ and $Ti_2Cu_3$ compounds at the Ti/filler metal interface and $TiAl_3$ compound as dark layer at the Ti/alumina interface. . . . .	55
4.17	$\alpha_2(Ag)$ phase on the filler area as bright region. . . . .	56
4.18	The layer of TiCu and $Ti_2Cu$ compounds at higher magnification. . . . .	56
4.19	All the interfaces and layers of intermetallic compound are observed into the joint area. . . . .	57
4.20	Layer of $Ti_3Al$ compound at the Ti/alumina interface and Bright layer of AlCu phase at the Ti/filler metal interface. . . . .	57
4.21	TiFe compound at the stainless steel/filler metal interface and some unknown ternary compounds are also observed next to this interface. . . . .	58

# List of Tables

4.1	Composition(at%) of the elements in the different layers of the brazed specimen, alumina/Fe, by using Ag-28Cu as the filler metal, taken by EPMA. . . . .	34
4.2	Composition(at%) of the elements in the different interfaces and layers of the brazed specimen, alumina/stainless steel, by using Ag-28Cu as the filler metal, taken by EPMA . . . . .	39
4.3	Composition(at%) of the elements in the different interfaces of the brazed specimen, alumuna/Nb, by using Ag-28Cu as the filler metal, taken by EPMA . . . . .	43
4.4	Composition(at%) of the elements in the different layers of the brazed specimen, alumina/Fe, by using Ag-27Cu-10In as the filler metal, taken by EPMA . . . . .	47
4.5	Composition(at%) of the elements in the different interfaces and layers of the brazed specimen, alumuna/Nb, by using Ag-27Cu-10In as the filler metal, taken by EPMA . . . . .	51
4.6	Composition(at%) of the elements in the different interfaces and layers of the brazed specimen, alumina/stainless steel by using Ag-27Cu-10In as the filler metal, taken by EPMA. . . . .	52

# Chapter 1

## Introduction

---

As the catalog of materials expanded, the technology of brazing increased and has been an enabling method for joining, used in the manufacture of many products. The process of brazing that we know today began as an ancient art. What began as art, however, evolved through our increased understanding of the nature and behavior of materials into art, technology, and science. Initially the development of materials progressed from the noble metals, gold and silver to copper, to the iron and steels, to the current range of, refractory metals, titanium, ceramics, composites and aluminides, while a parallel development occurred with braze filler metals. Initially filler metals were mixtures of metallic salts and organic reducing agents, however as time progressed, copper, brass and silver-copper base alloys were used heralding the filler metals of today and hopefully tomorrow. Concurrently the existing brazing processes and techniques were improved and new ones developed. These included direct and indirect methods of heating and the capability of controlling the ambient atmospheres which are all employed in the mass production applications of today.

The American welding Society [2] defines brazing as "a group of welding processes which produces coalescence of materials by heating them to a suitable temperature and by using a filler metal having a liquidus temperature above  $450^{\circ}$  C and below the solidus temperature of the base materials. The filler metal is dis-

tributed between the closely fitted surfaces of the joint by capillary attraction". This definition serves to distinguish brazing from other joining processes of soldering and welding. Brazing differs from soldering, by the term liquidus temperature, since soldering is performed below 450° C. On the other hand in welding, both filler metals and base materials are wetted during the process.

The uniqueness of the process is that metallurgical bonds are formed during brazing by melting only the filler metal and not the parts being joined. Both direct methods like diffusion bonding as well as indirect methods like brazing can be used to bond ceramics to ceramics or to metals and many process variations exist in both categories of bonding techniques. For example, in diffusion bonding many options exist for applying pressure and heat to the joint during the process. In some cases, diffusion bonding may employ an intermediate layer, which may or may not melt, as a bonding agent. Now a days brazing is a well established commercial process and is widely used in industry, in large part, because almost every metallic and ceramic material can be joined using this process. Generally brazing can easily be performed by manual techniques, but in future, it can just as easily be automated if necessary.

Ceramics are inorganic nonmetallic material that can be separated into two broad categories, traditional ceramics and structural ceramics. Traditional ceramics include clay products and refractories. The structural ceramic include monolithic materials such as aluminium oxide ( $Al_2O_3$ ), Zirconium oxide ( $ZrO_2$ ), Silicon carbide (SiC), Aluminium nitride (AlN), Silicon nitride ( $Si_3N_4$ ) and Silicon- Aluminium oxinitrides (SiAlON's). The technological interest in structural ceramics is directly related to their unique properties. This ceramic shows high strength not only at room temperature but also at elevated temperature. Besides high strength other properties that make ceramics attractive candidates for applications usually reserved for metallic alloys include excellent wear resistance, high hardness, excellent corrosion and oxidation resistance, low thermal expansion, and high electrical resistivity. For

these attractive properties these ceramics are being used to produce cutting tools, bearings, machine-tool parts, dies, pump seals, high temperature heat exchanger and turbine engine parts.

Although these ceramics provides a lot of attractive properties their brazing with metal or ceramics have their own inherent problems. Ceramic materials are inherently difficult to wet with conventional brazing filler metals. Most of the filler metals merely ball up at the joint and no wetting occurs. Another problem in brazing of ceramics results from the differences in thermal expansion between base material and the brazing filler metal and in case of ceramic to metal joints between the two base materials.

Alumina, Zirconia, beryllia, thoria, forsterite ( $Mg_2SiO_4$ ), Silicon carbide and nitride are the prime ceramic materials, which can be joined by brazing. Although a lot of research on alumina-metal and silicon carbide-metal brazing are going on but some of the problems still remain. A major problem with brazing an oxide ceramic is the resistance to wetting caused by the oxides on the surface of the ceramic. A means of rectifying the problem is to apply pressure to the braze filler metal with sufficient force to counteract the repelling force of the oxides. A study was undertaken to asses the strength of the joints of metals braze to alumina with Ti-containing braze filler metals by using both 94% and 99% alumina compositions. The results has shown that [1] higher strengths are observed when brazing took place in a vacuum and with the In-containing filler metal. A few researchers, for example [4, 7, 12, 13], focus on the most popular methods of obtaining seals between oxide ceramics and metals and compared the of joint strength of the two methods, namely Moly-Manganese process and Active brazing process.

More recently Byeong-joo Lee [5] developed a model for prediction of interface reaction products at  $Al_2O_3/Ti$  interface at  $1100^{\circ}C$ . It was reported that TiAl always forms first at the beginning of the interface reaction, but the stability of the TiAl depends on the oxygen potential in the Ti matrix. The effect of the initial Ti layer thickness on the stability of

the TiAl was also clarified [5]. Gubbels et al [6] have investigated a comparison between  $Ti-Al_2O_3$  diffusion bonding and titanium active brazing. In their work it was indicated that during brazing, first  $Ti-Al(O)$  intermetallics are formed. When the filler metal is depleted from Ti, the formed  $Ti-Al(O)$  intermetallics decompose in oxygen-saturated  $Ti(O)$  and Al, which in turn diffuses through the  $Ti(O)$  and dissolves in Ag.

A program was undertaken to evaluate active brazing to SiC because there is no suitable metallizing process available for this ceramic. Reactive wetting of Ag-Cu-Ti on SiC in *in-situ* high resolution transmission electron microscopy are focused in some research work. In this work it was reported [19] that SiC tend to dissolve along the (0001) plane and the reaction product adjacent to SiC was TiC. The crystallographic relationship between SiC and TiC was the same as that in bulk brazing.

Some researchers [22, 20, 21] are working on the decomposition and interfacial reaction in the brazing of SiC by copper-based active alloy. They concluded that that SiC could be decomposed easily by the Cu and Cu-5at%Ti alloy melt and in the brazing, three reaction layer were formed. These layers are copper/graphite, graphite/silicon, and copper silicides ( $Cu_7Si$ ) and  $Cu_3Si$ .

# Chapter 2

## Literature Review

---

### 2.1 Key Parameters Of Brazing

#### 2.1.1 Surface Energy and Surface Tension.

Before going to discuss the nature of wetting, contact angle, and spreading of liquid droplet over a solid, let us clear the concept of surface energy and surface tension. Fig [2.1] provides a simplified representation of the atomic structure of a solid close to one of its free surfaces.

The atom at position A in the bulk of the solid has a balanced array of neighboring atoms, whereas atom B at the surface of the solid is taking in neighbors above it, apart from the occasional vapor molecule, and thus has some unsaturated bonds. Thus the potential energy of atoms at the free surface, such as B, is higher than the energy of atoms within the bulk of the solids, such as A, by the energy of the unsaturated bonds. The aggregate of this excess energy that is possessed by atoms in the vicinity of the free surface constitutes the surface energy of the solid. On the other hand, surface tension ( $\gamma$ ) is defined as the force acting at right angles to a line of unit length(L) drawn in the surface i.e.  $F/L = \gamma$ . The surface energy is equivalent to surface tension under isothermal condition [2].

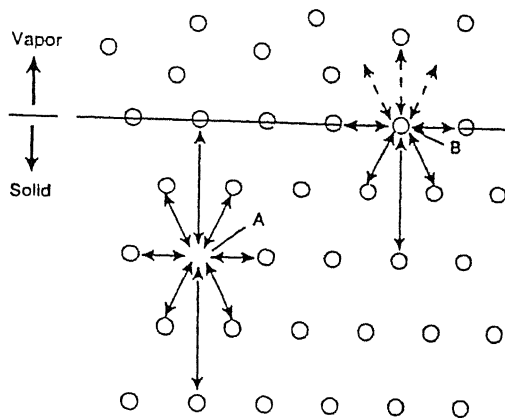


Figure 2.1: Simplified diagram of surface energies.

### 2.1.2 Wetting and Contact Angle

According to the classical model of wetting, the liquid will spread over a solid surface until the three surface tensions - between the liquid droplets and the solid substrate, the liquid droplet and the atmosphere, and the substrate and the atmosphere - are in balance as shown in Fig[2.2].

According to the balance of forces,

$$\gamma_{SL} = \gamma_{SV} - \gamma_{LV} \cos\theta \quad (2.1)$$

Where  $\gamma_{SL}$  is the surface tension between the solid and liquid,  $\gamma_{SV}$  is the surface tension between the liquid and the vapor,  $\gamma_{LV}$  is the surface tension between the liquid and vapor, and  $\theta$  is the contact angle of the liquid droplet on the solid surface. This equation is known as wetting equation. It shows that  $\theta < 90^\circ$  corresponds to the condition,  $\gamma_{SV} < \gamma_{SL}$ . This imbalance in surface tension provides the driving force for spreading of liquid over the solid surface and diminution of the unwetted surface area. The contact angle  $\theta$  provides a measure

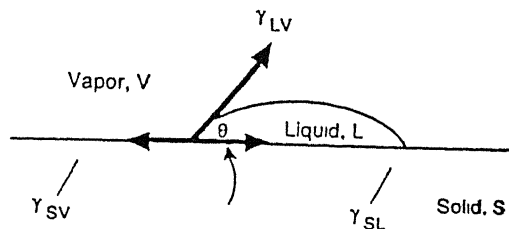


Figure 2.2: Surface tension forces acting when a liquid droplet wets a solid surface, according to the classical model. [2]

of the quality of wetting. Thus if  $90^\circ < \theta < 180^\circ$ , liquid will not be spread on the contacting surface. On the other hand, if  $\theta < 90^\circ$  liquid will wet the substrate and also spread. Therefore it is clear that area of spreading will increase with decreasing contact angle.

Rewriting the equation of contact angle  $\theta$ , as follows,

$$\cos\theta = \frac{\gamma_{SV} - \gamma_{SL}}{\gamma_{LV}} \quad (2.2)$$

Thus wetting is improved by decreasing  $\theta$ , which can be achieved by increasing  $\gamma_{SV}$ , decreasing  $\gamma_{SL}$  and  $\gamma_{LV}$ . The  $\gamma_{SV}$  can be maximized by cleaning the solid surface but  $\gamma_{SL}$  is highly temperature dependent and usually decreases rapidly with increasing temperature for a particular solid-liquid combination. Similarly  $\gamma_{LV}$  can be varied by altering the composition and pressure of an atmosphere used for the joining operation. This is one of the reasons for the popularity of vacuum-based joining process.

But in some cases, the wetting of surface is much more complex and use of classical model is not so simple, when chemical reaction between the filler metal and solid surface takes place. The effect of metallurgical interaction between filler metal and the component materials in promoting wetting is exploited in active filler metals, the addition of a small

fraction of a reactive metal such as Ti or Zr, to fillers which enables them to wet and spread over ceramic materials. In this instance, wetting of and reaction with ceramic are inextricably linked.

### 2.1.3 Fluid Flow and Factors Affecting the Fluid Flow

The liquid will flow into the joint under the force at a rate that is governed by its viscosity. Simple fluid flow theory assumes that, [1],

- There is no interaction between the liquid and the solid surfaces with which it is in contact.
- All surfaces are smooth and perfectly clean.
- Flow is laminar, not turbulent.

In this theory, the volume rate of liquid flow denoted as  $\frac{dV}{dt}$ , between a pair of horizontal parallel plates, length (l), separated by a distance (D), under a pressure (P) per unit area transverse to the plates is given as,

$$\frac{dV}{dt} = \frac{PD^3}{12\eta l} \quad (2.3)$$

where  $\eta$  is the viscosity of the liquid. It is assumed that the liquid front will advance at a rate  $\frac{dl}{dt}$  equal to the mean velocity of flow, that is

$$\frac{dl}{dt} = \left(\frac{1}{D}\right)\left(\frac{dV}{dt}\right) = \frac{PD^2}{12\eta l} \quad (2.4)$$

according to wetting equation, under isothermal conditions the change in surface energy as per unit area of a surface being wetted by the liquid is,

$$\gamma_{SL} - \gamma_{SV} = -\gamma_{LV} \cos\theta \quad (2.5)$$

Therefore the surface energy when the pair of parallel plates becomes wetted is

$$2l(\gamma_{SV} - \gamma_{SL}) = 2l(\gamma_{LV} \cos\theta) \quad (2.6)$$

the force (F) acting on the liquid to cause it to wet the plates is,

$$F = 2l \frac{\gamma_{LV} \cos\theta}{D} \quad (2.7)$$

So the velocity of flow of the liquid into the space between two parallel surfaces of separation (D), according this simple model is given by,

$$\frac{dl}{dt} = \frac{\gamma_{LV} D \cos \theta}{6\eta l} \quad (2.8)$$

Therefore according to this equation, rate of liquid flow increases when

- The liquid-vapor surface tension,  $\gamma_{LV}$  increases
- The joint gap, (D), increases
- The contact angle  $\theta$  decreases.

#### 2.1.4 Surface Roughness of Components

The roughness of joint surfaces can have a significant effect on the wetting and spreading behavior of a filler metal. It is well known that for each parent materials there is an optimum surface roughness for maximizing the spreading of the filler metals. Surface roughness reduces the effective contact angle  $\theta^*$ , where  $\theta^*$  is related to  $\theta$ , the contact angle for a perfectly flat surface, through the relation,

$$\cos \theta^* = r \cos \theta \quad (2.9)$$

where  $r = \frac{\text{actual area of rough surface}}{\text{plain area}}$ . At the same time, by producing a network of fine channels, the texturing may increase the capillary force acting between the filler and the component surfaces. If the texturing is too deep, the capillary dams can be formed and these will impede the spreading of the metal.

#### 2.1.5 Dissolution of Parent Materials by Molten Filler Metal

When filler metals are allowed to continue spreading beyond an initially wet surface area for longer time, the liquid flows into the joint will be associated with solid-liquid interfacial reactions, which are neglected in the fluid flow theory [3], due to which joint filling will be

sluggish at increased temperature and the viscosity of the molten filler metal will be reduced.

Dissolution of the substrate and resulting growth of intermetallic compounds both follow Arrhenius type rate relationships represented by,

$$RATE = \exp\left[\frac{-Q}{KT}\right] \quad (2.10)$$

where  $Q$  is activation energy at reaction temperature ( $T$ ). Interfacial reactions are important, not only in determining the flow characteristics of the filler and its wetting behavior but also the properties of the resulting joints. When a molten filler metal wets the parent material, there is normally some mutual solubility between them. It is usually manifested as dissolution of the surfaces of the parent materials in the joint region and the formation of new phases at either interface between parent materials and the molten filler metal or within the filler itself.

## 2.2 Prime elements of the brazing process

### 2.2.1 Temperature and time

The selection of an optimum braze temperature requires an understanding of the influence of temperature on both the wetting and flow of the filler metal, because the wetting and alloying action improves as the temperature increases. Of course, the temperature must be above the melting point of the brazing filler metal and below the melting point of the parent metal. Usually the lower brazing temperatures are preferred to minimize the heat effect on the base metal, base metal/filler metal interactions, and increase the life of fixtures or other tools. On the other hand, higher brazing temperature may be desirable for the filler metal of which higher melting temperature, for permitting subsequent processing at higher temperature, and effective removal of surface contaminants and oxides with vacuum brazing.

The brazing filler metal of complex alloys melted over a range of temperature. Therefore, for a particular temperature within that range, some constituents will be molten and the

higher melting constituents will remain solid. These would result in the separation of the lower melting constituents from the higher melting constituents of the filler brazing alloy and flow of this melted filler will be reduced for which the wetting and spreading tendency of the liquid phase will be hampered. The problem can be avoided by controlling the rate of heating and brazing time.

The time at the brazing temperature also affects the wetting action, particularly with respect to the distance of creep, of the filler metal. If the filler metal has a tendency to creep, distance generally increases with time.

### 2.2.2 Surface Preparation

A clean, oxide-free surface is imperative to ensure uniform quality and sound brazed joints. This can be achieved by removing all grease, oil, dirt and oxides or any other surface contaminants from base materials and filler metals before brazing, because only then can uniform capillary attraction be obtained. It is recommended that brazing should be done as soon as possible after the material has been cleaned. Otherwise unwanted surface contaminants may develop due to atmospheric conditions, storage, and handling practices. Usually cleaning is done in two ways, chemical cleaning and mechanical cleaning. Which cleaning process should be used, depends on the nature of the contaminant. Chemical cleaning is the most effective means of removing all types of contaminant.

On the other hand, surface roughness is also important in determining ease and evenness of flow of the braze filler metal in some cases. Generally, a liquid which wets a smooth surface will wet a rough one even more, because a rough surface will modify filler metal flow from laminar to turbulent, prolonging flow time and increasing the possibility of alloying and other interactions.

### 2.2.3 Joint Design and Clearance

A brazed joint is not a homogeneous body, it is a heterogeneous assembly composed of different materials with different physical and chemical properties. In a simplest case, it consists of the base material and braze filler metal. After brazing, a boundary zone will be formed between the base materials. Due to diffusion processes, the composition, physical, and chemical properties of that interface will be different from the base materials. This aspect should also be considered during joint design.

Clearance between base materials is also an important factor, because without clearance, the braze filler metal flow will be very restricted and results in voids or shrinkage cavities in the joint after solidification. Therefore a small clearance and thin filler metal films provides sound joint.

On the other hand, thermal expansion of dissimilar base materials is fundamentally important factor and complex. For example, in the ceramic to metal joining, there is a large difference of thermal expansion of ceramic and metal. During heating, the metal part will expand more than the ceramic part resulting in lesser clearance. During cooling, a stress field will develop in the interface region due to this thermal mismatch and results in poorer joint strength. Mizuhara et al [4] have investigated the effect of Ti concentration in the Cu-Ag filler alloy on the peel strength. Peel strength was observed to be maximum at a Ti concentration of about 1.5%wt. However, both below and above 1.5 wt pct Ti the peel strength was lower. According to them, plastic deformation of the brazing filler metal during cooling from the brazing temperature accommodates thermal expansion mismatch. Therefore, the increase in strength of the brazing filler metal that is due to excess Ti content leads to poorer accommodation of thermal expansion mismatch and results in high residual stress and hence low joint strength.

## 2.2.4 Source and Rate of heating

Heat must be supplied to the joint to raise the temperature of the filler metal and joint surfaces above the melting point of the filler metal. The joint surfaces need to be heated, otherwise the filler metal will be incapable of wetting them and will 'ball up'. To prevent this situation, it is good practice always to heat the filler metal via components to be joined and never vice versa. Two available methods of heating are used, first is the local heating, and second is the diffuse heating. In the local heating, only those parts of the components are heated which are in the immediate vicinity of the joint. But in the diffuse heating methods, the temperature of the entire assembly is raised, which results in the increasing process cycle time. On the other hand, there is less risk of thermal distortion, and easier accurate control of temperature.

Mizuhara et al [4] have suggested that in case of ceramic to metal joining, the heating rate is a critical factor, especially when the filler metal shows a strong alloying tendency with the substrate materials. For example, when Ag-Cu eutectic (72Ag-28Cu) is used to braze a copper substrate, copper readily dissolves into the Ag-Cu alloy. This leads to an increase in the melting temperature of the alloy. So a slow heating rate may result in a partial braze. It was also indicated [4] that a rapid heating rate is desirable in some cases, although this may not be possible when the ceramic member has a much higher mass than the metal member.

## 2.2.5 Joining atmosphere

For a molten filler metal to wet and bond to the base materials, the latter must be free from nonmetallic or oxides surface films. Although it is possible to ensure that this condition is met at the beginning of the heating cycle by prescribed cleaning treatments, significant oxidation will occur if the components are heated in air. Therefore steps must be taken to either prevent oxidation or remove the oxide film as fast as it forms by controlling the atmosphere surrounding the workpiece during brazing process. Usually three types of

atmosphere are possible, oxidizing, inert(vacuum), and reducing. In some joining process oxidizing process is desirable, such as Cu-copper oxide eutectic brazing process, in which copper is brazed to ceramic materials. A reducing atmosphere is one that is capable of chemically removing surface contaminants from the base materials. But there is some risk, when dealing with hydrogen, because of the hydrogen embrittlement and explosion at high temperature. On the other side, it is very difficult to create inertness or full vacuum during brazing process in the inert or vacuum atmosphere.

Mizuhara et al [4] have suggested that Ti readily reacts with oxygen, nitrogen, and water vapor in the brazing process. Consumption of Ti by interaction with the above depletes the amount of Ti available to wet the ceramic surface, and the reaction product can also form on the surface of the brazing filler metal which may prevent physical contact between Ti and ceramic part of the assembly. As a result, bonding with the ceramic will be poor. It was also indicated that, one of the best atmosphere for active brazing is a vacuum of level  $10^{-5}$  torr and leak rate of the vacuum furnace should be less than 0.67 Pa per hour.

### 2.2.6 Filler metal flow and their characteristics

The filler metal flow has a prime effect on the joint formation and its ultimate strength. Proper selection of filler metal provides more reliable and better joint strength. During filler metal flow, some complex metallurgical reactions may occur between base materials and the filler metal, which includes, carbide precipitation due to base materials effects, hydrogen embrittlement due to use of reducing atmosphere, heat affected zone may develop due to heating, vapor pressure over the filler metal effect, and alloying and stress cracking may take place due to base materials to filler metal interactions.

On the other side, filler metal characteristics is also an important aspect for better joint strength. It demands some metallurgical knowledge to produce brazing filler metals that would meet more specific needs. Some of the filler metal characteristics are listed below,

which are generally taken care to produce filler metals.

- Ability to form brazed joints with mechanical and physical properties suitable for the intended service application.
- Melting point or melting range compatible with the base materials being joined, and sufficient fluidity at brazing temperature to flow and distribute themselves into properly prepared joints by capillary action.
- composition of sufficient homogeneity and stability to minimize separation of constituents during brazing.
- Ability to wet surfaces of base materials and form a strong and sound bond.
- Depending on requirements, ability to produce or avoid filler metal interactions with base materials.

It should be pointed out that some specific alloy compositions known as eutectic do melt at one temperature rather than over a range of temperature. Therefore, melting characteristics may be an important consideration when selecting the brazing filler metal for a specific application.

## 2.3 Application of Phase diagram of Filler metals to Brazing

The phase diagram tells us about the ultimate balance of phases within the joint and those that are likely to be encountered during the progression towards equilibrium. A joined assembly in which the filler and abutting components are different materials are never in true compositional equilibrium, as long as the joint remains distinct. In most practical context, the composition of a joint will be tending toward equilibrium over most of its width, and therefore phase diagrams are applicable to an assessment of its constitution. However, at the edges of the joint, marked compositional gradients may exist, causing a significant deviation from equilibrium. Phase diagram can assist in the elucidation of metallurgical reactions and

resulting phases. Usually, the phase diagram gives us the following information.

- The melting temperature of the 'virgin' filler metal and of the abutting components.
- The probable freezing range of the filler metal following alloying with the components and hence the remelt temperature of the joint.
- Whether the filler alloy in the joint remains homogeneous after reaction with the components and, if not homogeneous, the phases that are likely to be present, or which may form subsequently, with their elemental compositional and melting temperatures.

### 2.3.1 Filler metals from binary alloy systems

A binary filler alloy with complete solubility in the solid state, used to join components of one of the constituent metals. Let us consider Au-Ni braze alloy used with nickel components. The Au-Ni phase diagram is given in Fig[2.3] [2], which shows this binary alloy system to posses a minimum melting point of  $955^{\circ}\text{C}$ , at 18%wt Ni. On either side of this composition, the liquidus and solidus boundaries separate, with the alloys melting over a range of temperature. Within the melting range, the alloy is partly liquid and partly solid. On cooling below the solidus temperature, an alloy of this system exists as a single phase solid, but as temperature is slowly lowered, this phase separates into two; one Au rich and the other Ni rich.

The temperature of decomposition varies with the composition, reaching a maximum of  $810^{\circ}\text{C}$  at 41.7%wt Ni as shown in the Fig[2.3]. The 18%wt Ni all alloy composition corresponding to the minimum melting point is normally used for brazing alloys, because it completely melts at a unique temperature.

A Au-50Ni is also used as brazing alloy. But the Au-Ni phase diagram shows that it has a solidus and liquidus temperature of  $1000^{\circ}\text{C}$  and  $1200^{\circ}\text{C}$ , respectively. Thus melting range of this composition is  $1000^{\circ}\text{C}$  to  $1200^{\circ}\text{C}$ , and brazing operation should be done above

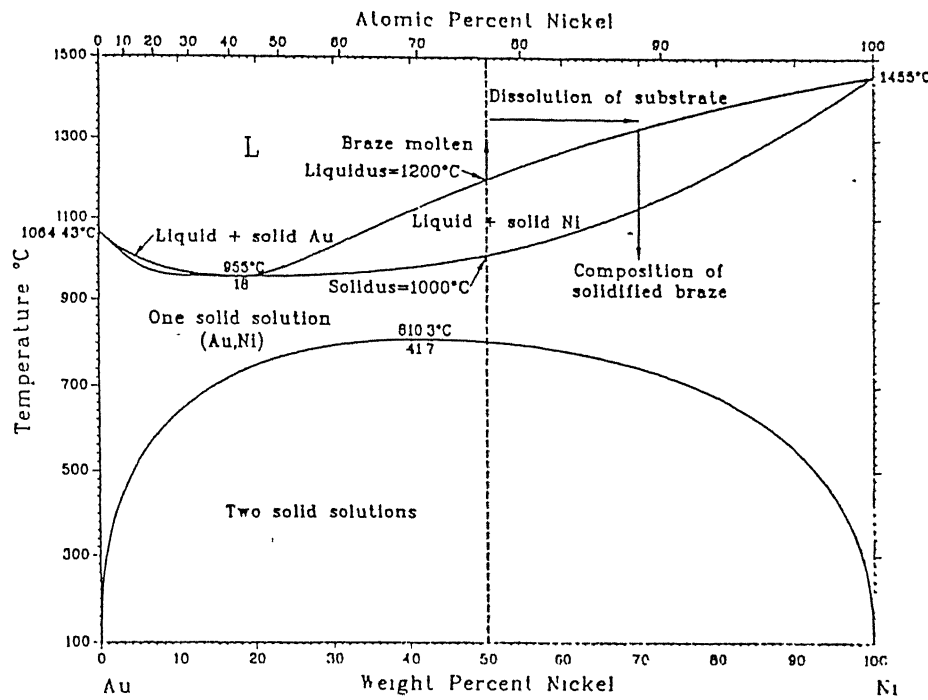


Figure 2.3: Au-Ni phase diagram. The erosion of a Ni substrate by a Au-Ni braze and the associated change to the composition of the filler metal are indicated.[2]

1200°C. On heating the braze above its liquidus temperature, the braze will wet and simultaneously dissolution of Ni substrate will take place. The composition changes to Au-70Ni approximately.

A binary eutectic composition braze used with components of one of the constituent metals with no intermetallic compound formation. A representative example of this type of reaction is a Ag-Cu braze used to join copper components. The Ag-Cu phase diagram is shown in Fig[2.4] [2]. Which shows that at a single composition i.e., eutectic,(Ag-28%wtCu), liquid phase will transforms to two solid phases at a unique

temperature, 779°C. Thus according the reaction,  $L = \alpha + \beta$ , at the eutectic composition, solid alloys form as a mixture of Ag rich( $\alpha$ ) and Cu rich( $\beta$ ) phases, and for all other compositions, the liquidus and solidus temperatures are separated from each other giving rise to solidification over a range of temperature.

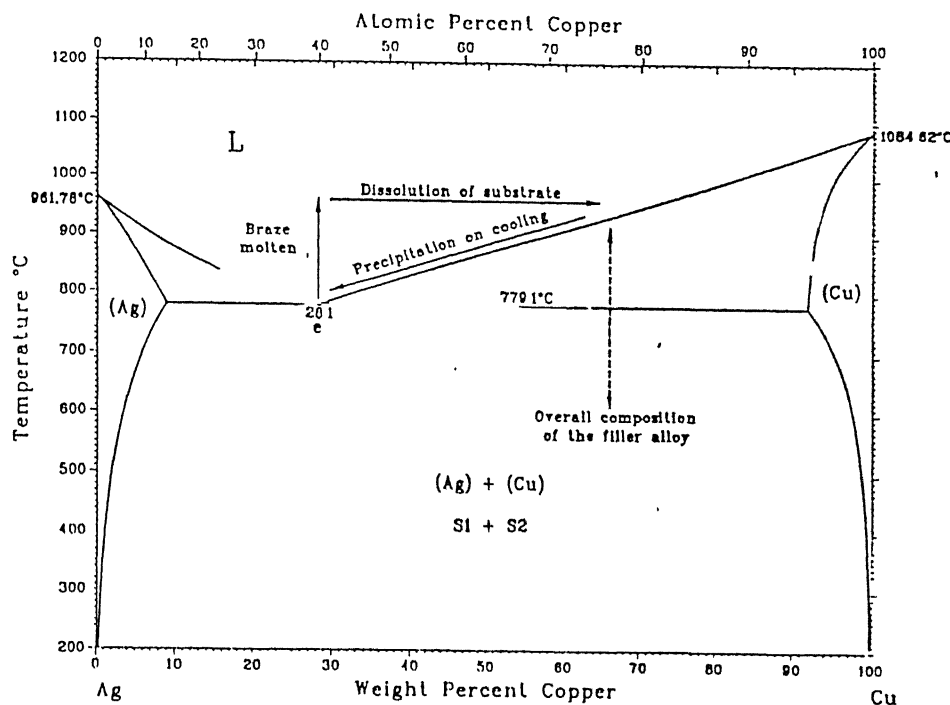


Figure 2.4: Ag-Cu phase diagram. Brazeing of copper components with Ag-28Cu eutectic braze results in dissolution of copper into the molten filler metal. [2]

At the joining process temperature, the braze will dissolve copper until equilibrium concentration of Cu is reached. In this case, dissolution of copper increases the liquidus temperature of the filler metal but not its solidus temperature because eutectic transformations are isothermal. On cooling below the liquidus temperature, the excess Cu-rich phase( $\beta$ ) will

solidify first this precipitation will occur preferentially at the components/filler metal interface because heat lost via extremities of the assembly provides the interface to be slightly cooler. The precipitation will continue until the temperature and the composition of the remaining liquid reach the eutectic point.

Generally eutectic alloys are preferred as filler metals because of the following characteristics,

- Superior spreading behavior when molten and melted at a unique temperature and not over a range of temperature.
- The duplex character and the fine grain size of the eutectic microstructure, provides enhancement of both the strength and ductility of a metal.
- Joining process temperature can be chosen to be only slightly above the melting point of the alloy.
- A rapid liquid to solid transformation on cooling, without intervening pasty stage and alloying of the filler metal does not greatly shift the composition from its eutectic point.

There are a number of braze metals such as Cu base alloys, Ag base alloys, and Au base alloys. They show superior brazing properties.

### 2.3.2 Filler metal from Ternary alloy system

It is not correct to say that only binary alloys are used as the filler metal. The ternary and multicomponent alloys are also used as filler metal in many cases. But in these cases, alloying does not result in the formation of new phases. More commonly intermetallic phases are formed. The volume distribution and morphology of these intermetallic phases has pronounced effect on mechanical properties of the joint. From a relevant phase diagram it is possible to predict whether the intermetallic compounds will form as a continuous interfacial layer against the parent materials or will be dispersed throughout the joint.

complete intersolubility between a eutectic braze and the metal on the joint surfaces. A typical example of this type reaction is provided by a Ag-28%Cu eutectic braze used in the fluxless brazing of Au-plated Mo component. For the three component system Ag-Cu-Au, ternary phase diagram is needed for the prediction of intermetallic compound that form in the joint.

The liquidus surface of the Ag-Au-Cu system is shown in Fig[2.5] [2].

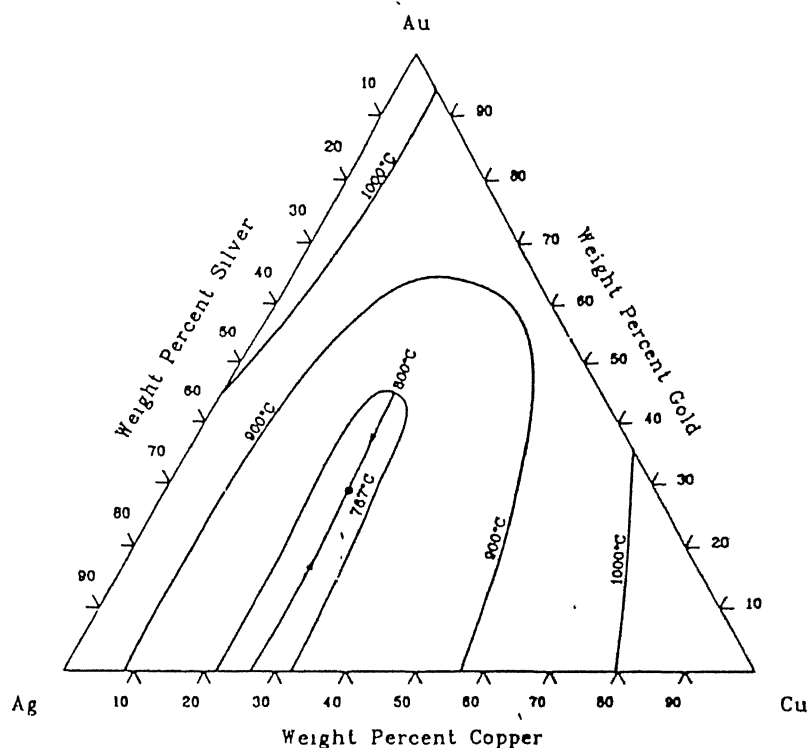


Figure 2.5: Liquidus surface of the Ag-Au-Cu ternary system. [2]

This surface contains a valley that runs from approximately the center of the diagram,

at the 800°C isotherm, to the eutectic point on the Ag-Cu binary axis. The minimum temperature in the valley is 767°C at a composition of 45Ag-29Au-26Cu. Fig[2.6] represents an isothermal section at 700°C, where the phases are solid [2].

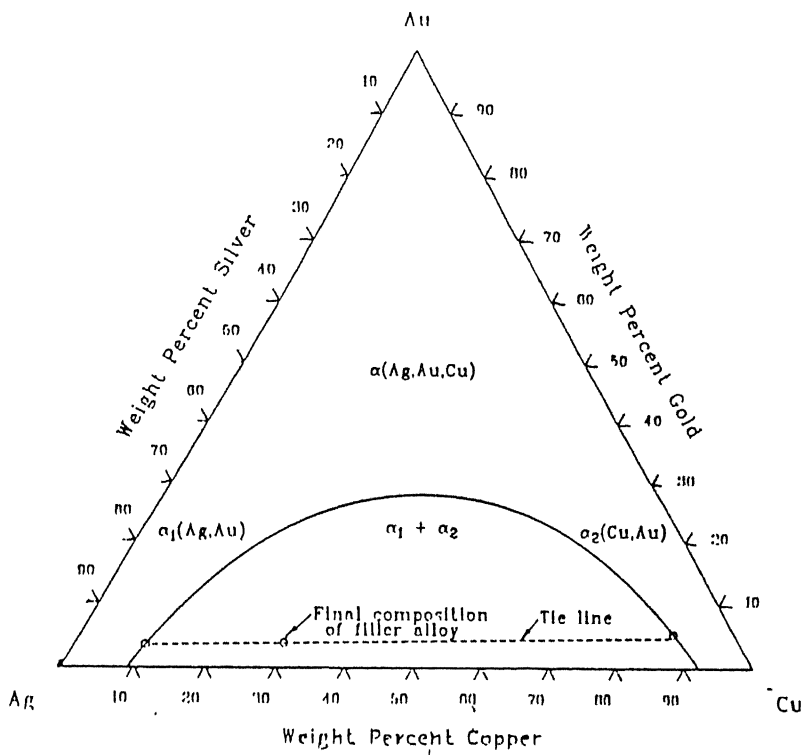


Figure 2.6: Isothermal projection of the Ag-Au-Cu phase diagram at 700°C A hypothetical tie line is shown linking the compositions of the two conjugate phases formed by the Ag-28Cu braze with a thin gold metallization. [2]

These comprises of two solid solutions, one is rich in Ag and Cu, and other is rich in Au, separated in the triangle by a parabolic boundary. Phase stability as a function of temperature is commonly represented by a diagram resembling a binary alloy phase diagram,

where either one of the constituents or the ratio of two constituents is held constant. When Au coating are used with the Ag-Cu braze alloy, the thickness of the Au layer will normally represent a maximum of about 2% of the volume of the metal in the joint. An Ag-Au-Cu phase diagram at 2%wt Au is shown in Fig[2.7] [2], because a single diagram can not be used to track the solidification sequence. In the joining operation, the molten Ag-28%wtCu braze fuses with the Au layer to form a single melt and consequently Mo will be wetted by molten alloy.

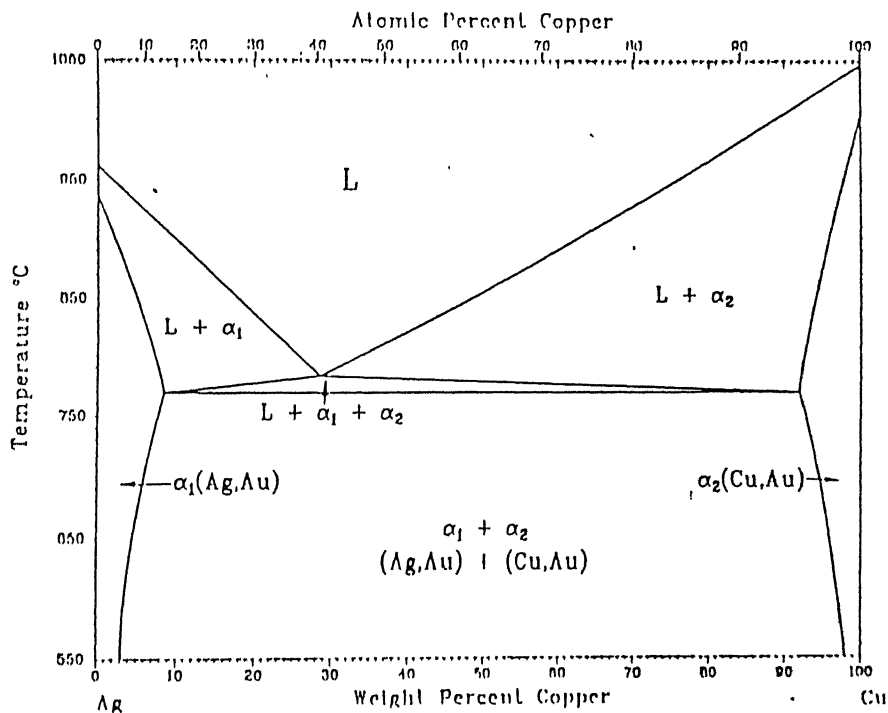


Figure 2.7: Schematic section through the Ag-Au-Cu ternary system at 2% Au. [2]

On cooling the liquid filler will solidifies to produce a eutectic microstructure comprising Ag and Cu rich phases, each containing some Au, as indicated in the Fig[2.7].

A number of filler metals of this type have been developed due to increasing application of brazing in different fields. Dissimilar combination of components such as ceramic to ceramic, ceramic to metal, glass to metal etc, can be joined by using these filler metals. Among them, Ag-Cu-In, Ag-Cu-Ti, Ag-Cu-Zn, Au-Cu, Ag-Ni-Pd are the leading usable filler metal for joining of ceramic to metal. A number of filler metal (both binary and ternary alloy) for brazing of ceramics are listed in the *Brazing Hand book* [3].

### 2.3.3 Reactive filler alloys

The wetting of nonmetallic components by commonly used filler metals is more difficult, but it can be accomplished by two practical routes, one of these is to apply metallization to the joint surfaces so as to render them essentially metallic in character. E.F Brush,jr et al [8] in their work have investigated that vapor coating of Ti and Zr on the alumina ceramic is very effective for enhancement of wetting, spreading, and capillary flow in brazing process and results in sound joints. They also studied Cr and Ca coating for wetting of alumina surface, which results in poor wetting and weaker joint strength. Mizuhara et al [14, 15] have investigated that instead of vapor coating of Ti on the alumina surface, Ti powder with an organic binder can be screened on the ceramic surface or very thin foil of Ti can be placed on the ceramic surface during active brazing process. Another approach involves incorporating small quantities of highly reactive elements into the filler metal.

When selecting a reactive filler alloy, the active ingredient should be optimum in concentration, appropriately processed, and must be reactive with the nonmetal. One of the most commonly used active constituents is Ti, which, when added to the Ag-Cu base brazing alloys, can facilitate wetting of the majority of engineering ceramics. There is often a wide temperature margin between the melting point of the activated filler and the its temperature of application. The process temperature is governed by the reactivity of the filler, which increases with temperature. Thus to prevent extensive erosion of the joint surfaces or growth

of the thick interfacial phases, the heating cycle should be kept short range, because the mechanical properties of the joint depends on the nature and morphology of the interfacial phases. These reactive filler alloys are primarily used for joining to engineering ceramics and refractory metals, namely oxides (alumina), carbides (SiC,WC), nitrides ( $Si_3N_4$ ,AlN) etc.

## 2.4 Wetting of ceramic materials

Usually ceramics are not wetted by most of the filler metals, even when their surfaces are scrupulously clean. This is because, they are chemically very stable, with their atoms strongly bound to one another. Therefore, the ceramics will not react with and be wetted by the filler unless it contains an active element that can attach itself to the anionic species of the ceramic material, which in a compound or complex is normally either oxygen, carbon, nitrogen or a halide element. The factors that govern the wetting of ceramics by active filler alloys should also be considered, because during wetting some chemical reaction occurs between active element and the ceramic surface. Thus, the behavior of the chemical reaction will also depend on the thermodynamic variables, such as Gibbs free energy, temperature, energy of the reaction, which should be taken into account to know about the nature of the reaction products.

### 2.4.1 Wetting and Interface reaction of Alumina( $Al_2O_3$ )

A major problem with brazing an oxide ceramic is the resistance to wetting caused by the oxide film on the surface of the ceramic. A means of rectifying the problem is to apply pressure to the braze filler metal with sufficient force to counteract the repelling force of the oxides. Nicholas et al [7] worked on the wettability of alumina by ternary alloys of Cu, Ti, and Al, gallium, Au, In etc. They concluded [7] that, the effect of increased Ti activity on wettability of alumina is not easy to asses since the free energy of  $Ti-Al_2O_3$  redox reaction is small and hence the chemistry of the ceramic surface is uncertain. It was also argued that

the Ti to oxygen ratio of the ceramic surface must increase with Ti activity and changes in interfacial chemistry affecting wetting behavior can also influence bond strength.

Brush et al [8] are worked on the wetting behavior of vapor coated alumina ceramics and concluded that, for a threshold thickness of Ti or Zr vapor coatings on alumina substrate effectively enhance wetting, spreading and capillary flow in brazing whereas the other metal coating such as Cr, Si germanium, Ni show lesser degree wettability. M.E Twentyman et al [9, 10, 11] has suggested that the high temperature metallization such as Mo and W paints are more effective for providing strongest seals between ceramic to metal. They have also indicated that, the commercial debased aluminas which were investigated contained a glass which were migrated at 1500°C and produced strong seals when the grain size of the alumina was suitably large.

Interface reaction of alumina ceramic to Ti or active filler alloy is an important aspect for the joining of ceramic to metal. Gubbels et al [6] in their work have compared between  $Ti-Al_2O_3$  diffusion bonding and Ti brazing process, and concluded that during active brazing with a Ag-4wt% Ti foil,  $Ti-Al(O)$  intermetallics are formed first at the ceramic surface. When the filler material is depleted, the intermetallic is converted to  $Ti(O)$  and Al, which in turn diffuses through the  $Ti(O)$  and dissolves in Ag. Li et al [5] have investigated the Ti-Al-O system, from which an isothermal section is shown in Fig[2.8] [5]. They reported that, in an infinite  $Ti-Al_2O_3$  diffusion couple the layer sequence is  $Al_2O_3/TiAl/Ti_3Al/Ti_2O/Ti$ , which leads to the diffusion path indicated in the phase diagram Fig[2.8]. In a finite symmetrical alumina-thick(Ti)-alumina sandwich diffusion couple, however, the layer is  $Al_2O_3/TiAl/Ti_3Al/Ti_2O/Ti_3Al/TiAl/Al_2O_3$ .

B.Lee et al [5] have indicated that  $TiAl$  always form first at the  $Ti/Al_2O_3$  interface when reacted at 1100°C, but the stability of  $TiAl$  begins to decrease when Ti matrix is saturated with oxygen and the  $TiAl$  layer that formed earlier transforms to  $Ti_3Al$ . The resultant layer sequence becomes  $(\alpha Ti)/Ti_3Al/Al_2O_3$ . However, when the initial Ti layer was thick, the

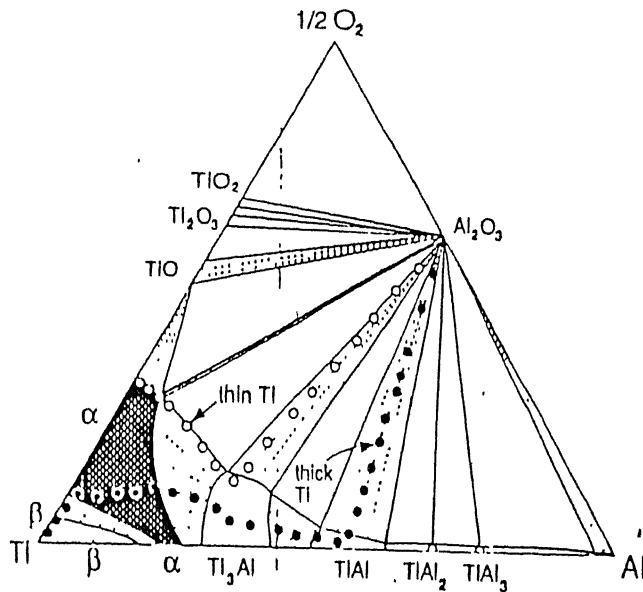


Figure 2.8: Isothermal section of the Ti-Al-O system at 1100°C and the diffusion paths between Ti and  $Al_2O_3$  in finite(thin) and infinite(thick) couples. [5]

saturation of Ti matrix with oxygen takes rather a long time, and TiAl can be observed resulting in the layer sequence  $(\beta Ti)/(\alpha Ti)/Ti_3Al/TiAl/Al_2O_3$  .

## 2.4.2 Reactive wetting and Interfacial reaction of SiC by Active filler metal

The reactive brazing of SiC involves many complicated bonding processes in which the ceramic dissolves in the molten alloy and many elements react together to form reaction products. Although the dissolution of ceramics and the nucleation and growth of reaction products are known the initial reaction kinetics has not yet been understood. Iwamoto et al

[19] have reported in their work, that, in case of SiC wetted by active filler metal (Ag-Cu-Ti), a series of chemical reaction takes place and results in the formation of TiC at the interface. The reaction can be written as,

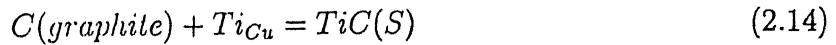


It was also suggested that[20], SiC lattice in contact with the molten Ag-Cu-Ti alloy initially dissolves with a few lattice planes along the (0001) plane and TiC epitaxially on the basal plane of SiC in the Si-C-Ti(-Ag-Cu) liquid phase. The TiC growth process was the rate- determining step and the TiC nanoparticles remain in the liquid phase when the SiC dissolution rate increases and TiC particles join together to form coarser particles.

H.K.Lee et al [22, 21] have investigated on the decomposition and interfacial reaction of SiC/Cu-5at% Ti interface. They have suggested that the formation mechanism of the reaction products in the interface was as follows:, the decomposition of SiC releases graphite and silicon rapidly



and Ti moves into the decomposition region and reacts with graphite to produce TiC at the side of SiC through the reaction



Simultaneously silicon dissolved in the copper melt, moves out of the decomposition region through the copper melt, and reacts with Ti to produce  $Ti_5Si_3$ .



Silicon released from the decomposition reaction also causes the brazing alloy to change from the copper phase to the copper silicides such as  $Cu_7Si$  and  $Cu_5Si$ . The formation of

the copper silicide depends on the brazing time, brazing gap and the presence of Ti in the filler metal.

# Chapter 3

## Experimental Procedure

---

The alumina ceramic circular disks used in this investigation were of very high purity(approximately, alumina powder was 99%+ pure). The circular ceramic disk was made by mixing of alumina powder with *polymer alcohol(PB)* binder and was pressed in cold condition into the  $\frac{1}{2}$  inch dia die by maximum pressure of 8 tones and was then sintered at 1500°C for 3 hours at horizontal tubular furnace.

The filler metals used were mainly Ag-Cu base eutectic alloys of composition 72Ag-28Cu and 63Ag-27Cu-10In, which were melted in silica capsules under vacuum. While making the filler metals, the melt was continuously stirred to ensure the formation of a homogeneous alloy and no segregation of the liquids. This alloy ingot was then cut into several discs to make the filler metal for the brazing process.

For the joining of ceramic to metal, the alumina, silicon carbide were used as ceramic member and stainless steel, niobium and pure iron were used as metal members. Titanium slice were used as an active metal for better wetting of ceramic surface. The metal members, stainless steel(12mm dia), niobium(6mm dia), pure iron(6mm dia) and titanium(10mm dia) had nearly circular cross section. A preliminary cut was made along the cross section using diamond cutter to make their surface flat. The Ti circular slice was thinned down to  $\frac{1}{5}$ th mm by grinding gently, for getting better wettability. This surface was then polished using

standard metallographic techniques to ensure optically flat surface for good bonding. The ceramic member ( $Al_2O_3$ ), filler metals (Ag-28Cu, Ag-27Cu-10In), and the metal member (stainless steel, niobium, pure iron) were also polished to ensure maximum area of contact between them and for getting effecting bonding. All the surfaces of the samples were then cleaned in ultrasonic cleaner to make sure that there is no unwanted particles on the surfaces which could hinder bonding.

The samples were then kept in an assembly as shown in Fig[3.1]. The sequence of the samples were as follows, the ceramic part was kept at the lowest position, on to which Ti slice was placed. It was followed by the filler metal and the metal part was at the top position. A graphite block was placed on the metal part and made screw tight. The graphite block were uscd to lower the oxygen potential and to separate the metal part from the screw.

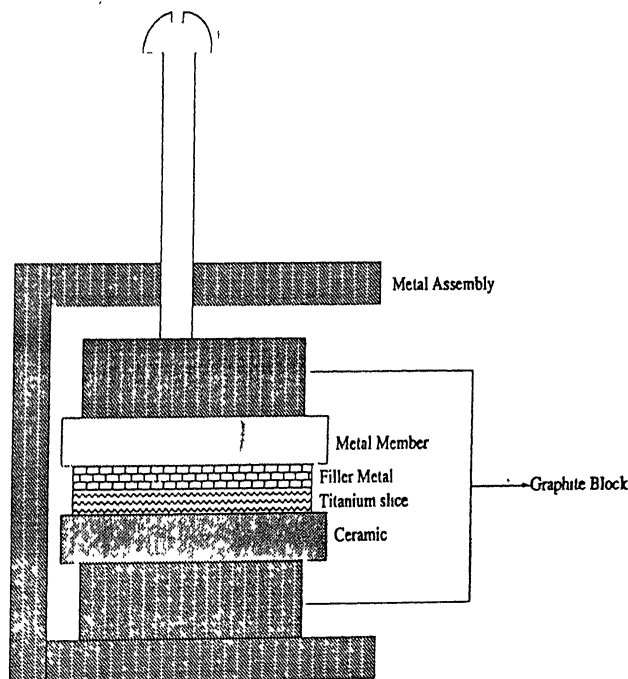


Figure 3.1: Section of the assembly in which the specimen were prepared.

The assembly was kept in a clean quartz tube and connected to a rotary vacuum pump. Vacuum of around  $10^{-3}$  to  $10^{-4}$  torr was obtained thereby ensuring little high temperature oxidation of the metals. The quartz tube was gently lowered inside a vertical furnace and kept at a fixed temperature.

The  $Al_2O_3$ /Ti/Ag-28Cu/stainless steel or Nb or Fe were kept at 900°C for 9 hours and 16 hours, and the  $Al_2O_3$ /Ti/Ag-27Cu-10In/stainless steel or Nb or Fe, diffusion couples were brazed at 800°C for 16 hours. The brazed samples were then air cooled keeping the vacuum pump running to ensure no oxidation and air entrapment in the liquid during cooling.

After joining of ceramic to metal the diffusion couple was cooled down to room temperature and cut with the help of a diamond cutter to expose the interfaces regions as shown in the Fig[3.2]. It was then mounted and polishing using the standard metallographic techniques.

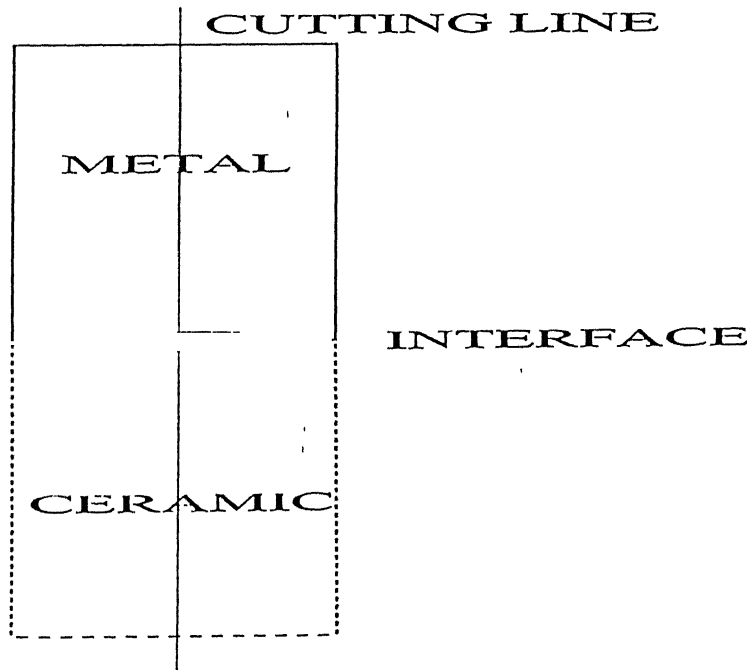


Figure 3.2: The line along which the brazed specimen was cut to expose the interface

The interface region was then studied using Electron probe microanalyser(EPMA) where the composition of the various phases were determined. Scanning Electron microscopy(SEM)

---

was also carried out on these samples to study the microstructure of various phases formed during solidification and the intermetallic layers.

# Chapter 4

## Results and Discussion

---

### 4.1 $Al_2O_3/Ti/Ag\text{-}28\text{Cu}/\text{Pure Iron(Fe)}$ System

The alumina ceramic was brazed with pure iron by using Ag-28%Cu binary alloy as filler metal and Ti as active metal, at 900°C for 16 hours. The results shows a complex microstructure due to presence of large numbers of element in the system. The microstructure can be explained by diffusion as well as chemical reaction mechanisms. In this system, the binary phases may appear in the microstructure from the Ti-Fe, Ti-Cu and Ag-Cu systems, and the ternary phases from the Ag-Cu-Ti, Al-Cu-Ti, and Ag-Cu-Fe systems. The compositions of different layers are derived by using EPMA as shown in Table[4.1].

#### 4.1.1 Phases from binary systems

As the experiment is carried out at 900°C, the binary phases will be formed during solidification from that temperature. Interfacial reactions take place at three interfaces, such as metal(Fe)/filler alloy, filler/Ti, and at the Ti/ceramic( $Al_2O_3$ ). As we scan the microstructure a number of interfaces and layers of intermetallic compounds formed as shown in the microstructure Fig[4.1]. In this system TiFe phase has formed at the Fe/filler metal(Ag-28Cu) interface. The microstructure also shows different morphologies of TiFe compounds,

Table 4.1: Composition(at%) of the elements in the different layers of the brazed specimen, alumina/Fe, by using Ag-28Cu as the filler metal, taken by EPMA.

SL. No.	Ag	Al	Cu	Fe	Ti	Identified Phases
1	0.068	0.016	0.000	99.90	0.006	Pure Iron
2	80.20	.507	17.38	1.89	0.00	Ag-rich Solution
3	5.35	0.56	5.06	41.48	47.52	TiFe
4	0.35	0.08	1.19	63.53	34.83	$TiFe_2$
5	79.50	6.53	13.22	0.47	0.26	Ag-rich Solution
6	56.34	4.63	38.48	0.27	0.23	Ag-Cu Eutectic
7	80.65	6.65	12.53	0.12	0.04	Ag-rich Solution
8	80.95	6.19	12.81	0.00	0.03	Ag-rich Solution
9	46.72	3.67	49.38	0.00	0.22	$(\alpha+\beta)$ mixture
10	4.89	2.53	23.68	12.83	56.04	Unknown Ternary phase

Fig[4.2]. The TiFe phase appears as a dark wavy layer at the Fe/filler metal interface. The compound  $TiFe$ , with  $CsCl$  structure forms from the melt by peritectic reaction ( $L + TiFe_2 = TiFe$ ) at  $1317^\circ C$ . The  $TiFe_2$  phase melts congruently at  $1427^\circ C$ . The  $(\alpha Ti)$  solvus is retrograde in form, and the maximum solubility of Fe in  $(\alpha Ti)$  is 0.05at%Fe at about  $700^\circ C$ . The maximum solubility of Ti in  $(\gamma Fe)$  is 0.8at% at approximately  $1150^\circ C$  as reported by J.L.Murry [23]. The  $TiFe_2$  phase forms as light region within the dark TiFe layer, Fig[4.2]. The  $TiFe_2$  is a  $MgZn_2$  type laves phase. Alloys of composition near  $TiFe_2$  are very reactive. It has been reported [23] that such alloy get contaminated by alumina crucible and for that, thoria had to be used. Ray [30] in his work, reported that  $(\beta Ti)$  solution contain 35 at% Fe, and TiFe from 35 to 50 at% Fe. The lattice parameters of the ordered and disordered phases follow a single linear trend with composition, from which he concluded that the metastable ordering transition may be a second order reaction.

The microstructure also shows that  $Ti_2Cu$  intermetallic forms at the Ti/filler metal interface, as dark region polyhedral light colored region, Fig[4.3]. Examination of Ti-Cu phase diagram [25] shows a number of intermetallic compounds in this system. The  $Ti_2Cu$  phase forms through the eutectoid reaction  $(\beta Ti) = (\alpha Ti) + Ti_2Cu$  at  $790^\circ C$  during cooling.

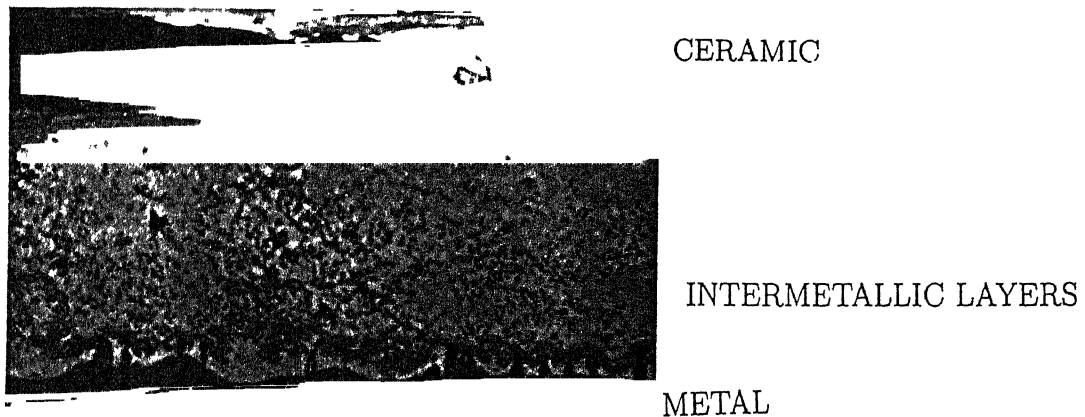


Figure 4.1.: All the interfaces and layers of intermetallic compounds in the joint area of the specimen

It is a stoichiometric compound, having  $MoSi_2$  type structure. The maximum solubilities of Cu in  $(\alpha Ti)$  and  $(\beta Ti)$  are 1.6 and 13.6 at% at 790°C and 1005°C, respectively. The maximum solubility of Ti in Cu is 8 at% at 885°C, as referred by J.L.Murry [25].

As we scan the solidification microstructure of the specimen, the different morphology of Ag-rich( $\alpha$ ) and Cu-rich( $\beta$ ) solid solutions are shown in Fig[4.3] and Fig[4.4]. The phase mixture appears as rod like eutectic with white region next to the metal/filler metal interface. The results taken by EPMA emphasized that in some position of the interface, Ag-Cu system forms as solid solution and in another position it shows exactly the eutectic composition without formation of any intermetallic compounds. From the Ag-Cu binary phase diagram [2], which shows a simple eutectic reaction, we can conclude that on cooling below the liquidus temperature, copper rich solid solution will solidify first and this precipitation tends to occur preferentially at the interface between the components and the braze, because this interface tends to be slightly cooler than the volume of the molten braze due to heat loss via the extremities of the assembly. Precipitation continues until the temperature and

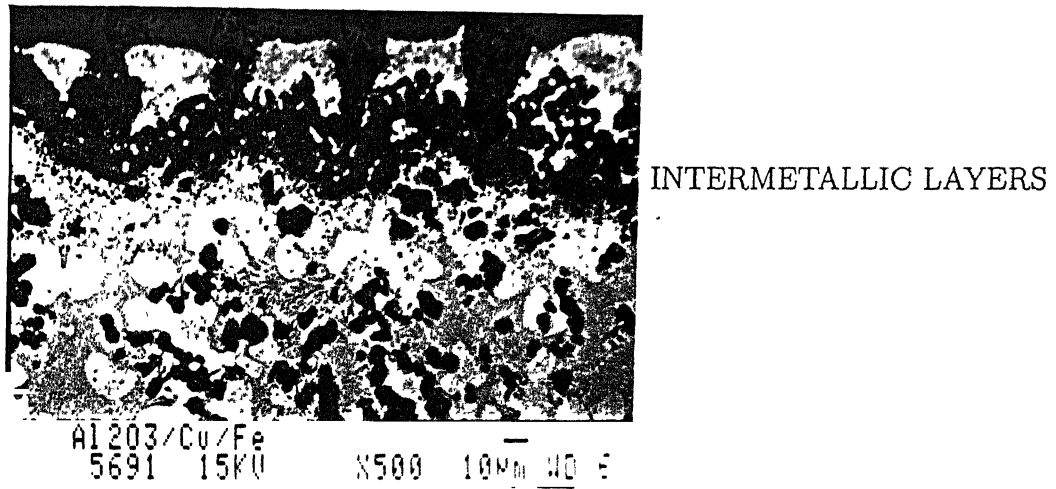


Figure 4.2: Different morphology of TiFe compound as a dark wavy layer at the Fe/filler metal interface

composition of the remaining liquid reach the eutectic point and forms a small volume fraction of the eutectic structure.

#### 4.1.2 Phases from Ternary systems

The result shows that some ternary phases form in the Ti/filler metal interface. The probable ternary systems are Al-Fe-Ti and Ag-Cu-Ti. The probable ternary phases are  $\tau_1$  ( $TiFe_2Al$ ),  $\tau_2$  ( $TiFeAl_2$ ) and  $\tau_3$  ( $Ti_8Fe_3Al_{22}$ ). The ternary phases are formed from binary Ti-Fe phases with some solubility for Al. The TiFe phase has 15 to 24 at% solubility for Al and hence increasing the lattice parameter of TiFe and form the ternary phase  $TiFeAl_2$ . As much as half of the Fe in the  $TiFe_2$  phase can be replaced by Al and change the lattice parameter of the  $TiFe_2$  phase and form the ternary compound  $TiFe_2Al$ . There are a number of ternary and binary intermetallic phases in the Al-Fe-Ti ternary system as seen in the isothermal section at 800°C [27]. Ghosh reported [27] that  $\tau_1$  phase has a cubic structure.

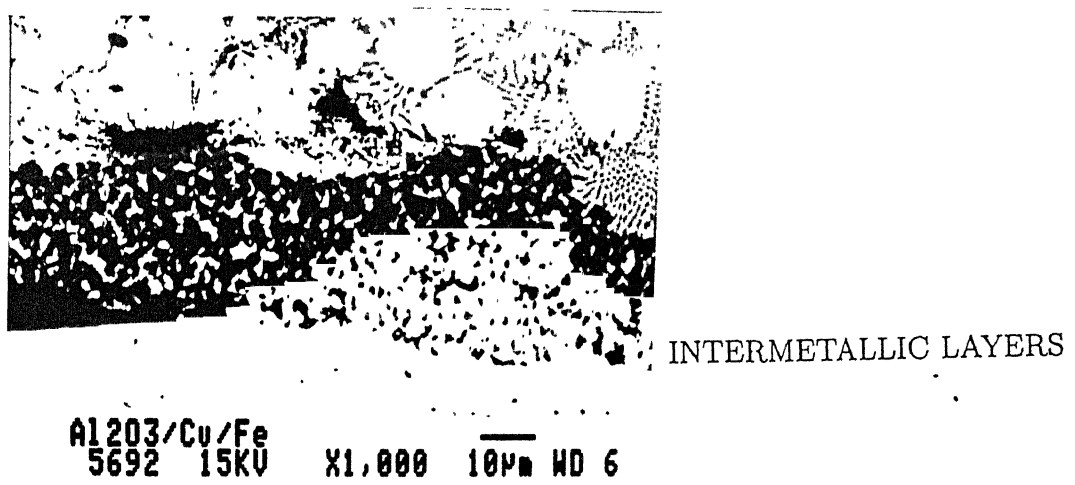


Figure 4.3:  $Ti_2Cu$  intermetallic compound forms as a polyhedral structure at the Ti/filler metal interface

The homogeneity range of the  $\tau_2$  phase at 800°C is from 40 to 50 at% Al at 24 at% Fe and the  $\tau_3$  phase has the composition  $Ti_{24}Fe_9Al_{66}$ .

In the Ag-Cu-Ti ternary system [26] no ternary compound has been reported. Only some intermediate binary phases of Ag-Ti and Cu-Ti systems are found. At the Fe/filler metal (Ag-28Cu) as well as the Ti/filler metal interface, as discussed in the previous section, the result did not show any Ag-Cu-Fe ternary phases at the Fe/filler metal interface. One unknown phase of Fe-Cu-Ti ternary system, has been found in the Ti/filler metal interface, Fig[4.3]. It is difficult to identify this phase as no ternary phase diagram of Fe-Cu-Ti is available at present. But if we consider the binary phases of Ti-Cu and Ti-Fe system then  $Ti_2Cu$  phase is the only possible phase that may form at this interface.

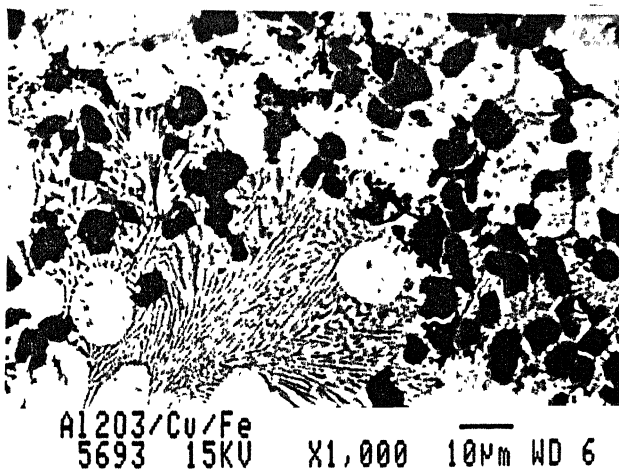


Figure 4.4: Different morphology of Ag-rich( $\alpha$ ) and Cu-rich( $\beta$ ) solid solution

## 4.2 $Al_2O_3/Ti/Ag-28Cu/Stainless\ Steel(Fe-Ni-Cr)$ System

The alumina ceramic was brazed with 18-8 stainless steel by using the Ag-28Cu binary alloy as a filler metal and Ti as the active metal at 900°C for 9 hours. The microstructure appears to be complex due to the presence of a large number of elements in the system. The composition of different elements taken from different positions of the diffusion couple are shown in Table[4.2].

Most of the identified phases appear to belong to the binary systems, such as Ti-Fe, Ti-Cu, and Ti-Ag. At some positions of the diffusion couple, ternary phases of the Fe-Cr-Ti, Fe-Cu-Ti and Ag-Cu-Ti systems appear in the microstructure, Fig[4.5].

Table 4.2: Composition(at%) of the elements in the different interfaces and layers of the brazed specimen, alumina/stainless steel, by using Ag-28Cu as the filler metal, taken by EPMA

SL. No.	Ag	Al	Cu	Cr	Fe	Ni	Ti	Identified Phases
1	79.95	6.16	13.21	0.00	0.00	0.00	0.66	Ag-Cu Solid Solution
2	43.36	3.84	49.28	0.00	0.00	0.00	3.49	( $\alpha$ + $\beta$ ) mixture
3	7.05	3.45	39.88	0.02	0.03	0.00	49.52	TiCu
4	2.73	4.85	9.22	0.00	0.14	0.11	82.92	( $\beta$ Ti)
5	3.73	3.81	43.17	0.04	0.13	0.38	48.71	TiCu
6	46.55	0.46	48.44	0.05	0.22	0.02	4.25	( $\alpha$ + $\beta$ ) mixture
7	85.55	0.46	13.51	0.00	0.16	0.00	0.30	Ag-rich Solution
8	85.17	0.37	14.10	0.00	0.00	0.05	0.05	Ag-rich Solution
9	0.95	3.49	31.97	0.84	11.22	2.98	48.53	(TiCu + $Ti_2Cu$ )
10	50.92	0.99	28.37	1.00	5.57	0.35	12.78	TiCu + Ag matrix
11	2.87	0.18	0.92	23.03	55.90	1.12	15.95	Unknown Ternary phase(Fe-Cr-Ti)
12	0.06	0.07	0.49	25.98	66.19	2.69	4.90	( $\alpha$ Fe)
13	0.00	0.00	0.17	19.50	72.82	7.47	0.02	18-8 Stainless Steel
14	0.02	0.02	0.04	20.02	72.97	6.89	0.02	18-8 Stainless Steel

#### 4.2.1 Phases from Binary systems

From the compositional data taken by EPMA and solidification microstructure, it is confirmed that  $TiCu$ ,  $Ti_2Cu$  binary phases form at the  $Ti$ /filler metal interface, Fig[4.5]. The solubilities of Cu in Ti and their formation mechanism are discussed in the section 4.1. As we scan the microstructure of the sample, the  $Ti_2Cu$  phase forms as dark cuboid particle layer at the  $Ti$ /filler metal( $Ag-28Cu$ ) interface, Fig[4.6]. The  $TiCu$  phase forms at the Stainless steel/filler metal( $Ag-28Cu$ ) interface as dark wavy layer, Fig[4.5].

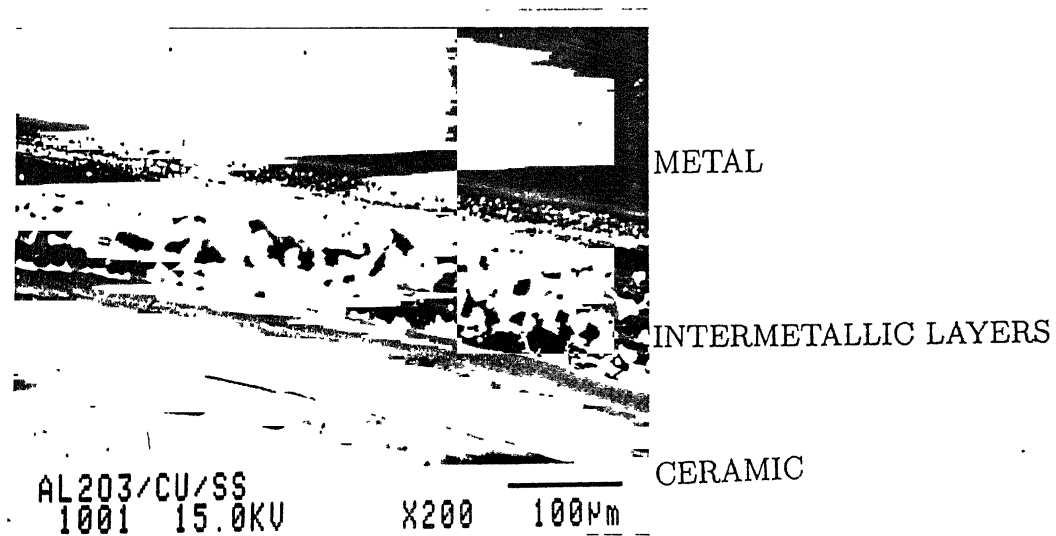


Figure 4.5: All the interfaces and layers of intermetallic compound at the joint area. .

The result shows inadequate data for the  $Ti$ - $Ag$  phase formation. The microstructure also shows some  $Ag$ - $Cu$  rod-like eutectic structure, Fig[4.7]. The structure forms simply by the eutectic reaction at  $779^{\circ}C$  during solidification from  $900^{\circ}C$ . The 18-8 stainless steel contains 18% Cr and 8% Ni, which may allow us to consider binary and ternary phases from the  $Ti$ -Cr and  $Ti$ -Fe systems. The  $Ti$ /ceramic( $Al_2O_3$ ) interface composition indicates ( $\beta$  $Ti$ ) formation, which has a bcc structure. Lee et al [5] has indicated that there will form

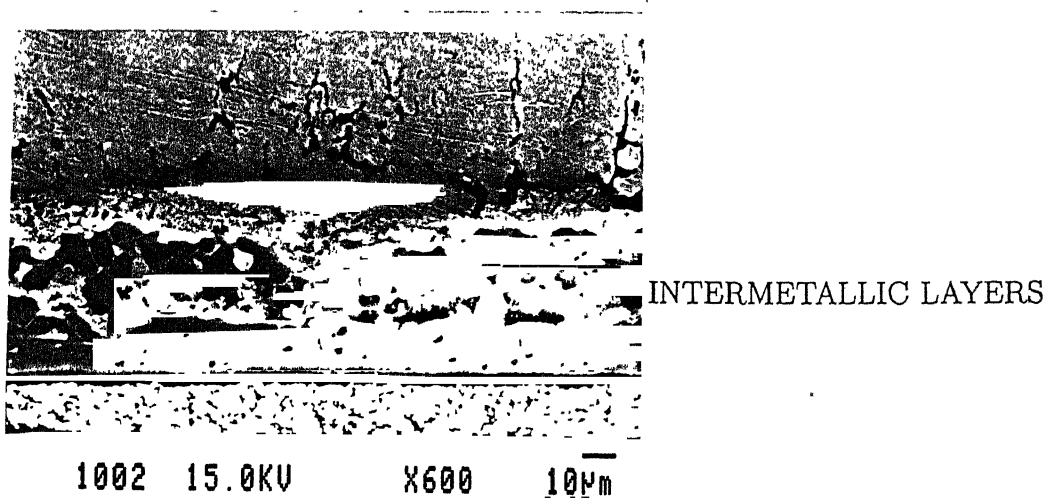


Figure 4.6: Morphology of  $TiCu$  and  $Ti_2Cu$  intermetallic compound at the  $Ti$ /filler metal interface.

a metastable phase boundary between  $Ti$  and  $Al_2O_3$ , at higher temperatures before the formation of interfacial reaction products.

#### 4.2.2 Phases from Ternary systems

No ternary compound from the  $Fe-Cr-Ti$  system has been observed. There are two binary phases,  $TiCr_2$  and  $TiFe$  forms with some solubility for other elements. These phases form next to the stainless steel/filler metal interface with distinct wavy intermetallic layer, Fig[4.5]. If we examine the phase diagram of the  $Ti-Cr$  system, the  $TiCr_2$  phase forms through the eutectoid reaction  $(\beta Ti) = (\alpha Ti) + TiCr_2$  at  $670^\circ C$ . It is difficult to identify the crystal structure of  $TiCr_2$  phase. The morphology and reaction mechanism of  $TiFe$  phase has already discussed in the previous section.

No ternary compound of the  $Ag-Cu-Ti$  system has been found and only the binary phase  $TiCu$  is observed in the  $Ag$  matrix as dark particles, Fig[4.6]. Simultaneously compositional

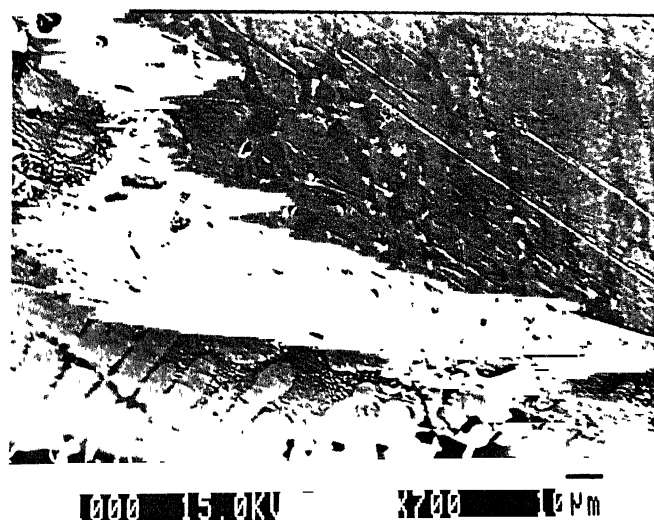


Figure 4.7: Eutectic structure of solid solution.

data of EPMA shows a ternary compound of the system Fe-Cu-Ti. But as no reliable ternary phase diagram of Fe-Cu-Ti is available, it is difficult to analyze the phases formed by the system.

### 4.3 $Al_2O_3/Ti/Ag-28Cu/Pure Niobium(Nb)$ system

The alumina ceramic was brazed with pure Niobium by using Ag-28Cu alloy as the filler metal and Ti as the active metal at  $900^{\circ}C$  for 9 hours. As the experiment was carried out at low temperature ( $900^{\circ}C$ ), the wetting of Nb was inadequate due to higher melting point of Nb. Nevertheless, some binary phases have formed in the diffusion couple. The compositions of element present at different positions of the diffusion couple are shown in Table[4.3]. The phases are mainly derived from Ti-Cu, Ti-Ag and Ag-Nb binary system.

The phases are mainly derived from Ti-Cu, Ti-Ag and Ag-Nb binary system.

Table 4.3: Composition(at%) of the elements in the different interfaces of the brazed specimen, alumina/Nb, by using Ag-28Cu as the filler metal, taken by EPMA

SL. No.	Ag	Al	Cu	Nb	Ti	Identified Phases
1	0.00	0.05	0.00	99.95	0.00	Pure Niobium
2	43.55	3.39	52.04	0.04	0.95	( $\alpha+\beta$ ) mixture
3	58.78	4.19	8.18	23.92	4.27	Unknown Ag-Nb phase
4	46.30	4.04	48.58	0.00	1.06	( $\alpha+\beta$ ) mixture
5	0.29	9.42	38.48	1.16	50.63	TiCu
6	42.10	3.13	25.15	0.35	29.26	TiCu + Ag matrix
7	0.24	8.88	38.75	1.21	50.89	TiCu
8	0.69	11.20	35.31	1.46	51.32	TiCu

#### 4.3.1 Phases from Binary systems

The compositional data and microstructure shows that the TiCu phase form into the Ag matrix as a dark particle with wavy layer at the Ti/filler metal interface, Fig[4.8]. The TiCu phase forms through the reaction  $L = TiCu$  at  $985^{\circ}C$ . This phase has  $B_{11}$  structure, with a homogeneity range of 48 to 52 at% Cu and melts congruently at  $985^{\circ}C$ . With increasing at% of Cu and lowering of temperature, the TuCu phase goes through the peritectic reaction  $L + TiCu = Ti_3Cu_4$  at  $925^{\circ}C$  to give the  $Ti_3Cu_4$  phase.

An unknown binary phase of Ag-Nb system has also been found from the compositional data and the microstructure, Fig[4.9]. This phase appears as bright spheroidal particles at the Nb/filler metal interface. At some positions of the interface, a mixture  $\alpha$  and  $\beta$  phases of the Ag-Cu system forms by eutectic reaction because the Ag-Cu of the eutectic composition produces simply Ag-rich( $\alpha$ ) and Cu-rich( $\beta$ ) phases during solidification from the liquid state. Fig[4.10] shows rod-like nature of Cu rich( $\beta$ ) phase in a fine dispersion of the Ag-rich  $\alpha$  matrix.

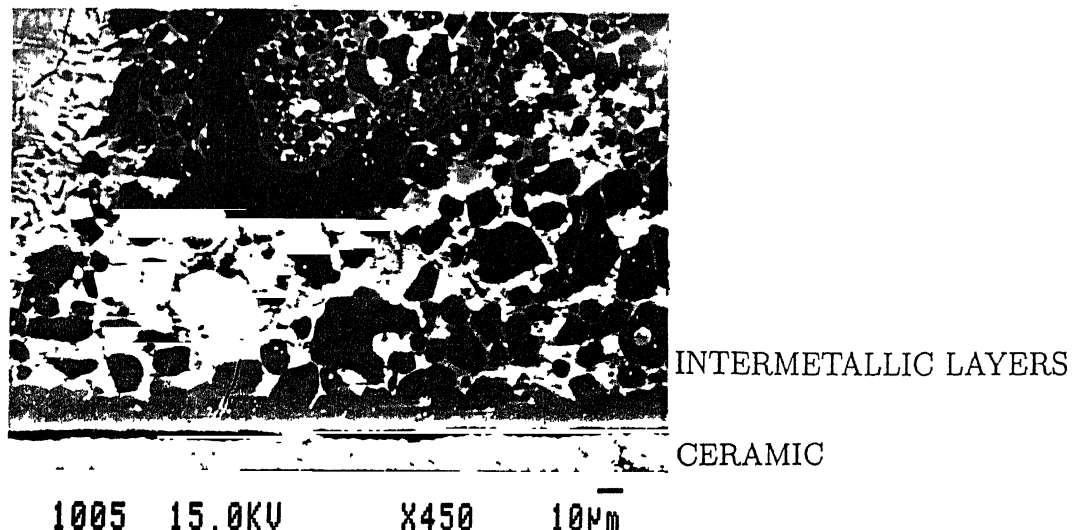


Figure 4.8: TiCu intermetallic compounds into the Ag matrix as a dark particle.

#### 4.3.2 Phases from Ternary systems

One compositional data are matched with ternary composition of Ag-Cu-Ti system. This unknown phase has been observed a white region next to the Ti/filler metal interface as we scan the solidification microstructure of the specimen. Kubaschewski has reported [26] that there is no ternary compounds in the Ag-Cu-Ti system but the intermediate phases may appear mainly from the Ti-Ag and Ti-Cu systems. From the study of Ti-Ag phase diagram, it can be confirmed that this bright region is nothing but a TiCu dark phase in a Ag-rich matrix, Fig[4.8]. Kubaschewski has also indicated [26] that at 700°C the Ag solid solution is in equilibrium with all the phases which exist at this temperature, except Ti, TiCu and TiAg. Although, TiCu and TiAg phases are isothermal but not in equilibrium to each other.

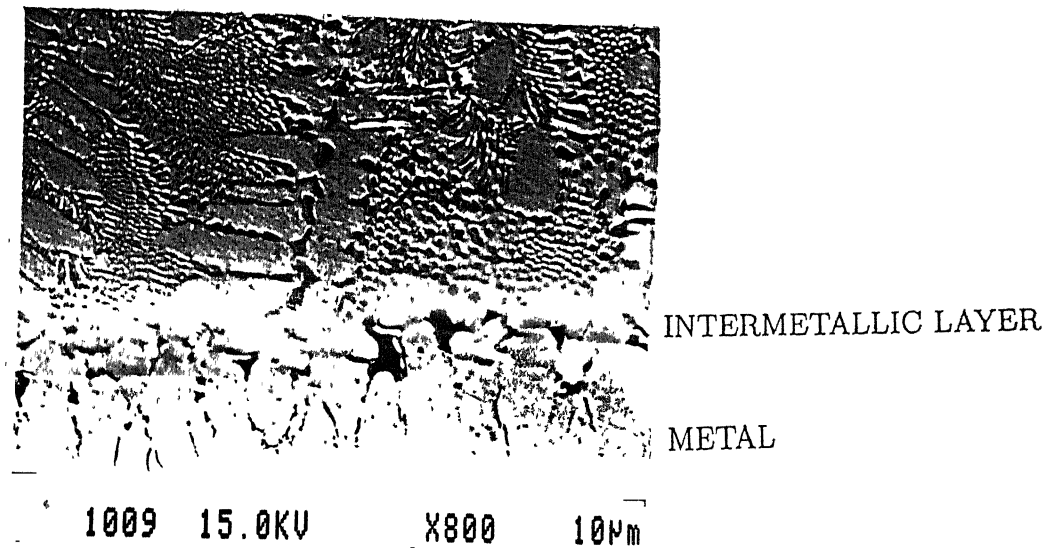


Figure 4.9: Unknown phase from Ag-Nb system as a spheroidal particle.

## 4.4 $Al_2O_3/Ti/Ag\text{-}27Cu\text{-}10In/Pure Iron(Fe)$ system

The alumina ceramic was brazed with pure iron by using the Ag-27Cu-10In alloy as the filler metal and Ti as the active metal at 800°C for 16 hours. Due to large number of element present in the system, a complex microstructure results. The compositional data is given in the Table[4.4]. A number of intermetallic compounds are formed as shown in the microstructure of Fig[4.11]. The intermetallic compound layer that form at the interfaces are mainly from Ti-Cu and Ti-Fe binary systems. Some ternary compositions are also observed.

### 4.4.1 Phases from Binary systems

The  $TiFe_2$  binary phase have been found as a dark continuous layer next to the pure iron as can be seen from the microstructure, Fig[4.12]. From the study of the Ti-Fe diagram,  $TiFe_2$  phase form through the reaction  $L = TiFe_2$  by congruent allotrophic transformation. Similar to the compositional data of section [4.1] the  $TiFe$  intermetallic compound is observed

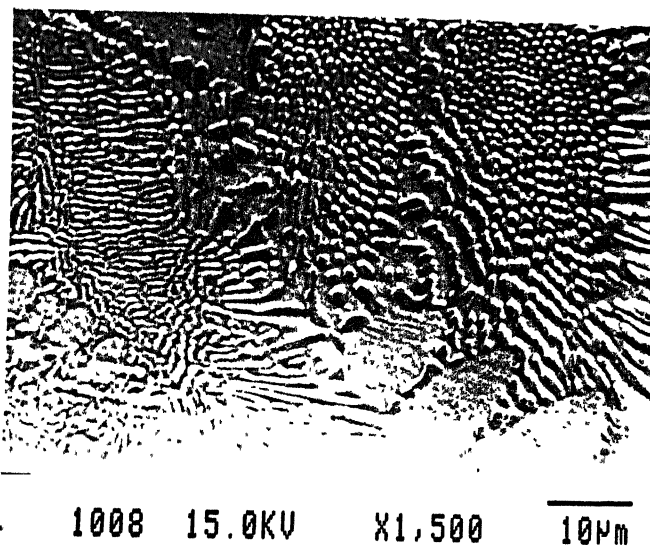


Figure 4.10: Rod-like nature of Cu-rich  $\beta$  phase in the Ag matrix( $\alpha$ ).

at the Ti/filler metal interface. Generally this phase form through the peritectic reaction  $L + TiFe_2 = TiFe$  at  $1317^{\circ}C$ . The microstructure, shown in Fig[4.13], shows the small dark layer of  $TiFe$ , as confirmed by the results. The binary phase  $Ti_3Cu_4$  from the Ti-Cu system has been found next to Fe/filler metal interface through the peritectic reaction  $L + TiCu = Ti_3Cu_4$  at  $925^{\circ}C$ .

This phase forms as dark particles within the white region near the interface, Fig[4.13]. The Cu present in the Ag-Cu alloy comes in contact with the Ti and forms dark  $Ti_3Cu_4$  particles. This phase is a stoichiometric compound and having similar crystal structure with  $Ti_2Cu_3$  and  $Ti_2Cu$ . The eutectic structure of the Ag-Cu ( $\alpha+\beta$ ) are also seen in this diffusion couple. But in this system, no rod-like structure of the Ag-Cu eutectic has been observed.

Table 4.4: Composition(at%) of the elements in the different layers of the brazed specimen, alumina/Fe, by using Ag-27Cu-10In as the filler metal, taken by EPMA

SL. No.	Ag	Al	Cu	Fe	In	Ti	Identified Phases
1	0.00	0.00	0.05	99.92	0.00	0.02	Pure Iron
2	39.55	3.34	44.26	1.21	6.83	4.80	( $\alpha+\beta$ ) mixture
3	0.06	0.07	0.66	64.78	0.02	34.41	$TiFe_2$
4	49.38	4.14	28.23	1.09	16.85	0.28	Ternary phase(Ag-Cu-In)
5	41.69	6.89	46.64	0.32	4.42	0.01	( $\alpha+\beta$ ) mixture
6	3.24	0.38	54.53	0.06	1.73	40.03	$Ti_3Cu_4$
7	37.64	5.95	52.02	0.27	4.12	0.00	Ag-Cu eutectic
8	42.74	1.65	50.92	0.11	4.54	0.34	„
9	52.07	4.72	34.64	2.85	6.01	0.17	„
10	66.37	5.59	11.72	5.72	9.97	0.83	Ag-rich solution
11	6.76	1.90	3.09	39.61	0.97	47.66	$TiFe$
12	0.08	99.51	0.00	0.35	0.00	0.63	$Al_2O_3$ Ceramic

#### 4.4.2 Phases from Ternary systems

Although some compositional data gives the ternary composition, but no ternary intermetallic compounds appears to have found in this diffusion couple.

### 4.5 $Al_2O_3/Ti/Ag-27Cu-10In/Pure Niobium(Nb)$ system

The alumina ceramic was brazed with pure niobium by using Ag-27Cu-10In ternary alloy as the filler metal and Ti as the active metal at 800°C for 16 hours. The composition of the element in the different layers, taken by EPMA are shown in Table[4.5].

A large number of intermetallic compound are observed from the Ti-Cu binary system at the Ti/filler metal interface. An intermetallic compound of the Ti-Al system forms at the Ti/ceramic( $Al_2O_3$ ) interface. An unknown intermetallic compound of Ag-Cu-Ti system is also observed. The microstructure of layers that form in the diffusion couple is shown in Fig[4.14].

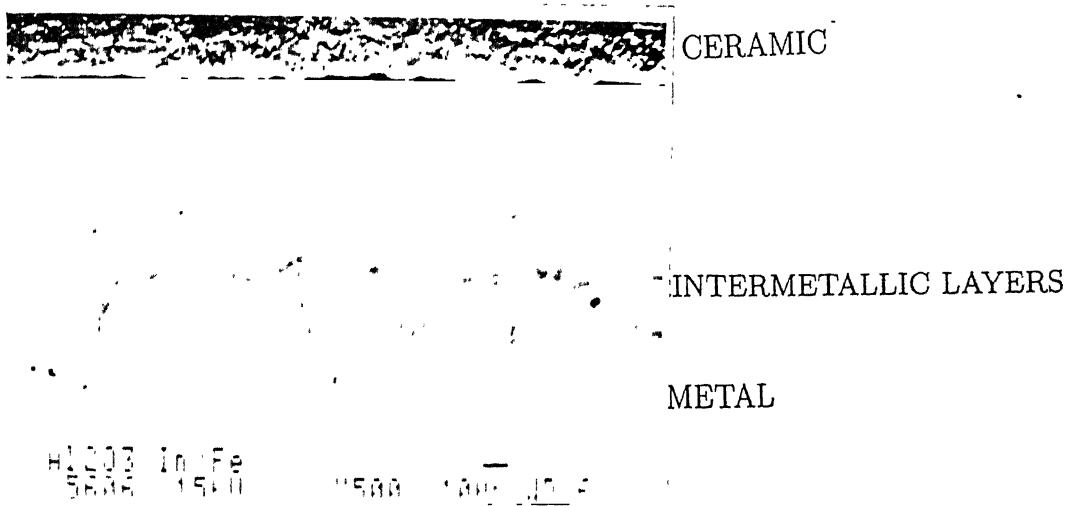


Figure 4.11: All the interfaces and layers of intermetallic compounds formed into the joint area of the specimen.

#### 4.5.1 Phases from Binary systems

The microstructure shows that the  $TiCu$  phase forms next to pure niobium at the  $Nb$ /filler metal interface as a dark region, Fig[4.15], Fig[4.18]. According to the  $Ti$ - $Cu$  phase diagram [25] this phase forms through the eutectic reaction  $L = Ti_2Cu + TiCu$ . The  $Ti_2Cu$  phase also formed in this diffusion couple but near the active metal/filler metal interface. The  $Ti_3Cu_4$  stoichiometric compound formed as a bigger dark particle in the light matrix of  $Ag$ , Fig[4.15]. The  $Ti_3Cu_4$ ,  $Ti_2Cu_3$  and  $Ti_2Cu$  intermetallics are formed at the  $Ti$ /filler metal interface, Fig[4.16]. Between the congruent melting point of  $TiCu$  and the eutectic reaction at 73 at%  $Cu$ , there is a cascade of peritectic reactions involving the compounds  $Ti_3Cu_4$ ,  $Ti_2Cu_3$ ,  $TiCu_2$ , and  $TiCu_4$ . These intermetallic compounds forms as single layers next to the active metal( $Ti$ ), Fig[4.14]. The  $TiAl_3$  intermetallic compound from the  $Ti$ - $Al$  system is observed at the  $Ti$ /ceramic( $Al_2O_3$ ) interface as dark layer, Fig[4.16]. The  $TiAl_3$  is

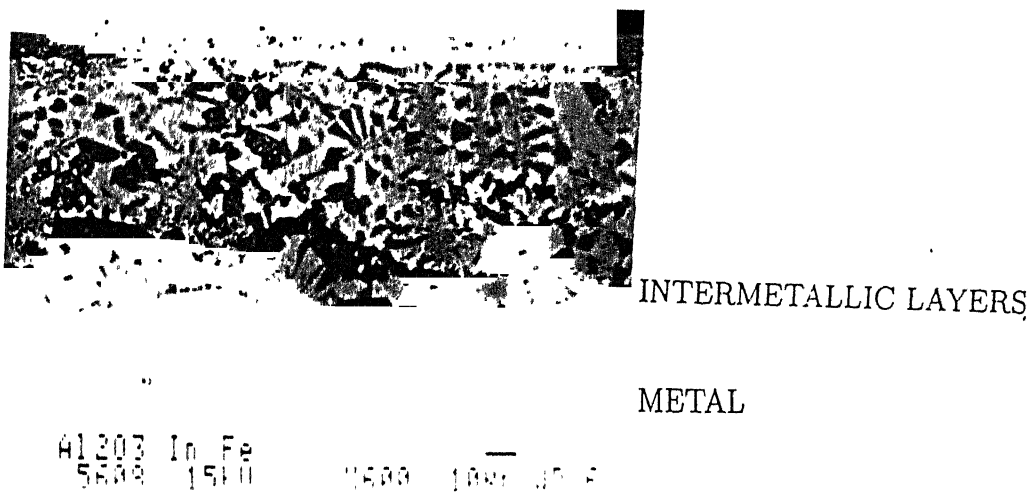


Figure 4.12: Structure of  $TiFe_2$  phase as a dark continuous layer next to the pure iron.

a stoichiometric compound with  $DO_{22}$  ordered fcc structure.

This phase forms through the peritectic reaction and at lower temperatures it transforms to  $\alpha TiAl_3$  phase. J.L.Murry has reported [23], the formation of this intermetallic compound. The  $TiCu_4$  phase has been reported by Bru [29] and Gie [28].

#### 4.5.2 Phases from Ternary systems

The compositional data also shows some ternary phase composition of Ag-Cu-In and Ag-Cu-Ti systems in some position of the diffusion couple. As no ternary compound formation is reported for both these systems, it is difficult to identify the ternary compounds. In the case of Ag-Cu-In ternary system, the Ag content is higher and the Cu and In content is inadequate to form the ternary phases from this system. From the study of the ternary phase diagram [31] of Ag-Cu-In, it can be confirmed that the phase is nothing but an  $\alpha_2$  (Ag) phase as seen in the microstructure, Fig[4.17].

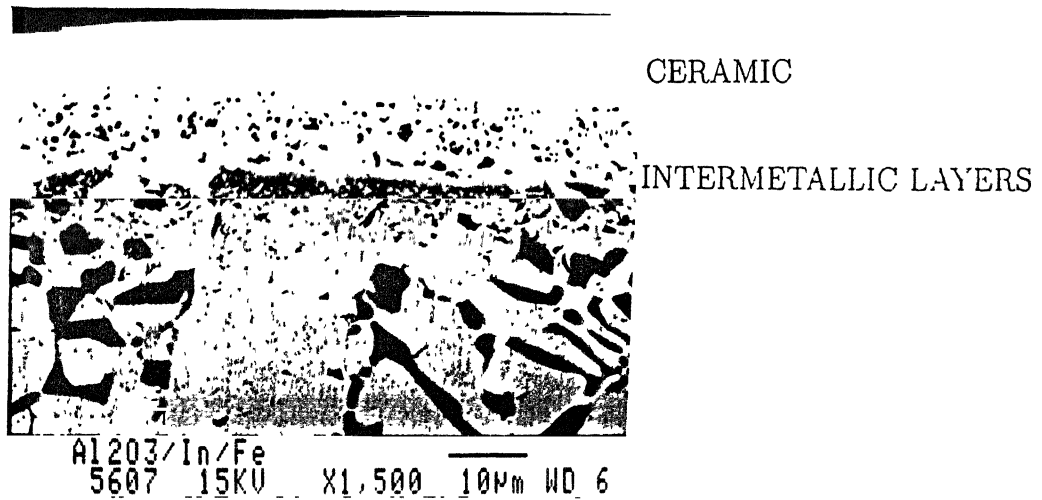


Figure 4.13: TiFe phase as a small dark layer at the Ti/filler metal interface.

It is observed as a bright region on the filler metal. Kubaschewski et al [31] has reported that the  $\gamma_1$  ( $Cu_7In_3$ ) phase occurring at high temperatures in the Cu-In system, forms a solid solution with the low temperature  $\gamma_2$  ( $Ag_9In_4$ ) phase of the Ag-In system and the bcc high temperature phases of the Cu-In system ( $\beta_1$ ) and  $\beta_2$  of Ag-In system both get stabilized in the ternary and decompose eutectically at 490°C and 475°C respectively. In case of Ag-Cu-Ti system, no ternary compound has been reported. Binary phases from Ti-Cu or Ti-Ag systems may form, as intermediate phases, at the interface. As the Ag and Cu content is more or less the same and the Ti content is inadequate to form the binary phases of the Ti-Cu and Ti-Ag, it appears to be an unknown ternary compound of Ag-Cu-Ti system. This phase form as a white layer at the Ti/filler metal interface, Fig[4.16].

Table 4.5: Composition(at%) of the elements in the different interfaces and layers of the brazed specimen, alumuna/Nb, by using Ag-27Cu-10In as the filler metal, taken by EPMA

SL. No.	Ag	Al	Cu	In	Nb	Ti	Identified Phases
1	0.10	0.63	0.15	0.03	99.08	0.00	Pure Niobium
2	71.19	5.26	11.48	10.84	0.00	1.20	Ag-rich Solution
3	1.53	0.17	53.51	0.11	1.19	43.48	$Ti_3Cu_4$
4	4.76	0.42	47.31	0.43	0.65	46.42	TiCu
5	2.04	0.17	52.17	0.73	1.04	43.83	$Ti_3Cu_4$
6	2.02	0.23	52.78	0.11	0.00	44.83	$Ti_3Cu_4$
7	53.85	4.26	22.83	13.99	0.00	5.03	$\alpha_2$ phase
8	18.46	1.87	47.71	3.99	0.00	27.93	$Ti_2Cu_3$ + Ag matrix
9	24.09	1.89	52.33	2.71	0.00	18.96	TiCu <sub>4</sub> + Ag matrix
10	33.21	3.01	32.46	6.28	0.00	25.01	Unknown phase(Ag-Cu-Ti)
11	1.09	6.03	38.29	0.42	0.00	53.68	$Ti_2Cu$
12	0.42	8.00	35.49	0.40	0.00	55.68	$Ti_2Cu$
13	2.32	72.85	0.94	0.45	0.00	23.42	TiAl <sub>3</sub>
14	0.26	98.90	0.40	0.14	0.00	0.28	$Al_2O_3$

## 4.6 $Al_2O_3/Ti/Ag-27Cu-10In/Stainless Steel(Fe-Cr-Ni)$ system

The alumina ceramic was brazed with 18-8 stainless steel at 900°C for 9 hours. As the experiment was carried out at a higher temperature than the liquidus temperature of the Ag-27Cu-10In alloy, the filler metal spread well over the ceramic and resulted in better wetting of the metal surface. The compositional data taken by EPMA are shown in the Table[4.6]. The important intermetallic compounds form mainly from the Ti-Fe, Ti-Al, binary systems and from the Fe-Cr-Ti, Ag-Cu-Ti, Fe-Cu-Ti, Al-Ag-Cu and Al-Cu-Ti ternary systems. The microstructure, Fig[4.19] contains a huge number of intermetallic layers.

Table 4.6: Composition(at%) of the elements in the different interfaces and layers of the brazed specimen, alumina/stainless steel by using Ag-27Cu-10In as the filler metal, taken by EPMA.

SL. No.	Ag	Al	Cu	Cr	Fe	In	Ni	Ti	Identified Phases
1	0.04	0.06	0.17	20.12	72.07	0.00	7.48	0.03	18-8 Stainless Steel
2	0.11	0.24	0.65	23.81	63.79	0.04	2.32	9.02	( $\alpha$ Fe)
3	22.05	0.23	7.55	9.31	33.02	4.46	1.59	21.76	Unknown phase
4	3.88	6.79	16.47	0.30	22.72	0.84	9.73	39.23	Intermetallic layer
5	0.54	2.53	8.87	0.44	30.99	0.20	7.91	48.47	TiFe
6	47.07	3.96	42.32	0.00	0.40	5.41	0.04	0.78	( $\alpha+\beta$ ) mixture
7	1.34	2.02	6.21	2.94	23.33	0.34	6.52	57.27	( $\beta$ Ti)
8	41.60	9.24	41.90	0.05	0.16	7.14	0.00	0.28	Ag-Cu eutectic
9	30.06	39.04	24.54	0.11	0.84	3.95	0.00	1.42	Ternary phase of Ag-Al-Cu
10	36.08	4.55	50.90	0.16	1.58	5.49	0.12	1.09	Ag-Cu eutectic
11	1.50	17.18	9.36	1.48	10.89	0.38	5.28	53.91	$Ti_3Al$
12	0.18	18.02	10.77	0.80	7.60	0.17	5.52	56.91	$Ti_3Al$
13	0.05	98.65	0.10	0.12	0.92	0.00	0.06	0.06	$Al_2O_3$ Ceramic

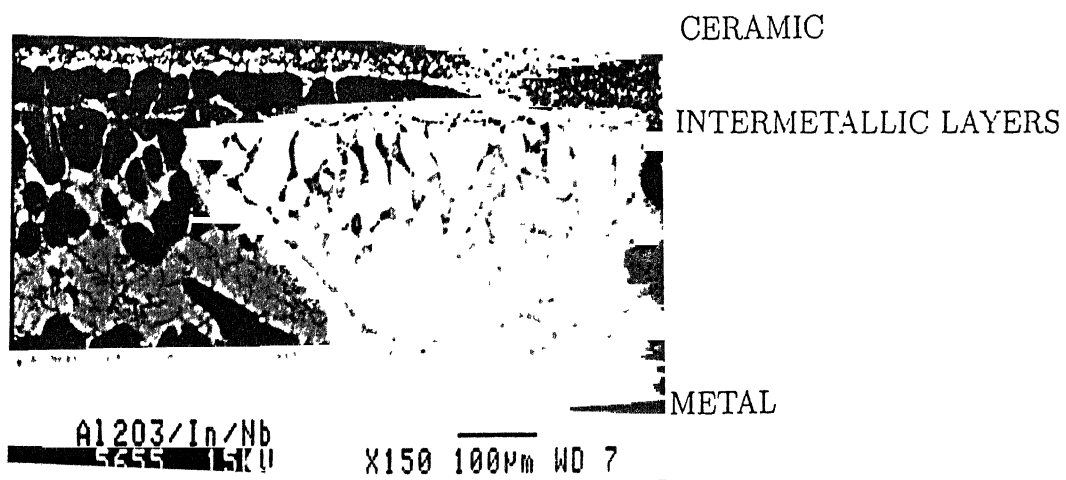


Figure 4.14: All the interfaces and layers of intermetallic compounds into the joint area.

#### 4.6.1 Phases from Binary systems

The  $TiFe$  phase has formed in this system at the stainless steel/filler metal interface, Fig[4.21]. It has formed through the peritectic reaction  $L + TiFe_2 = TiFe$  at  $1317^{\circ}C$ , but remains stable at lower temperatures. The binary phase  $Ti_3Al$  from the Ti-Al system formed at the Ti/ceramic( $Al_2O_3$ ) interface as a thin dark layer, Fig[4.20]. This phase is an ordered hexagonal structure based on  $\alpha$ Ti (cph) and forms through the reaction  $(\alpha Ti) = Ti_3Al$  towards the alumina side. B. Lee has reported [5] that after saturation of  $\beta$ Ti matrix with oxygen present in the  $Al_2O_3$ , the Ti/ceramic( $Al_2O_3$ ) interface composition moves towards low Al and high oxygen direction on the metastable  $\beta$ Ti/TiAl phase boundary between the two initial phases with interfacial reaction time. The stability of TiAl is expected to decrease as the interface composition moves toward low Al and high oxygen direction, while the stability of  $Ti_3Al$  would be increased. After the saturation of Ti matrix with oxygen, the TiAl layer would transform to  $Ti_3Al$  layer in reaction time. The Ag-Cu eutectic structure

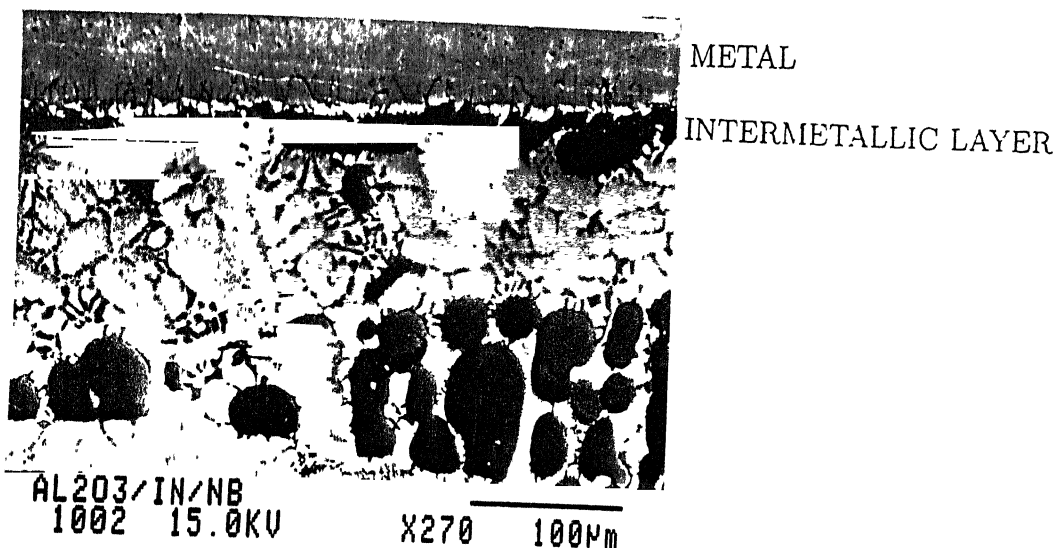


Figure 4.15: Layer of  $TiCu$  compound at the Nb/filler metal interface and the particle of  $Ti_3Cu_4$  compound at the light matrix of Ag are shown.

$(\alpha+\beta)$  has also been observed in this case.

#### 4.6.2 Phases from Ternary systems

At the stainless steel/filler metal interface, the compositional data shows the Fe-Cr-Ti ternary composition. As the Cr and Ti contents are insufficient to form any ternary as well as binary compounds, it is confirmed from the study of the ternary phase diagram that  $\alpha$ Fe is the dominating phase in this case. An unknown ternary compound is found as a dark layer at the stainless steel/filler metal interface. This compound has also been found in some other position of the interface as a dark particles as shown in Fig[4.21]. But as the Ti content appears to be dominating in this case, it can be concluded that  $(\beta Ti)$  is the feasible phase. A new unknown intermetallic compound from the Al-Ag-Cu system, has been observed at the Ti/filler metal interface as a bright layer as shown in the microstructure of Fig[4.20]. As the Al and the Ag contents are dominating in the Al-Ag-Cu system, it may be a binary

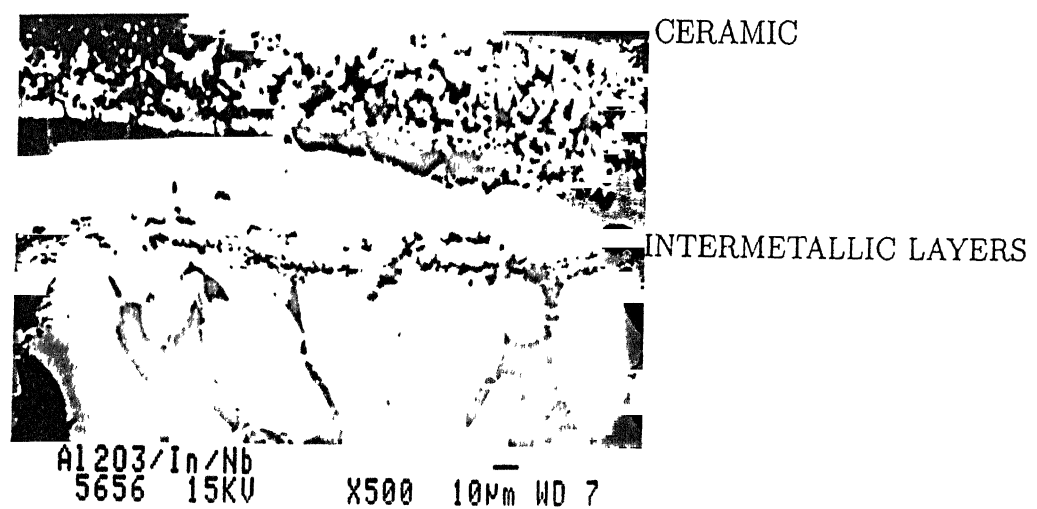


Figure 4.16: Layer of  $Ti_2Cu$  and  $Ti_2Cu_3$  compounds at the Ti/filler metal interface and  $TiAl_3$  compound as dark layer at the Ti/alumina interface.

compound of the Al-Cu system. It is most probably the AlCu phase [24]. A dark layer of ternary phase Ag-Fe-Ti forms next to the stainless steel, Fig[4.21].

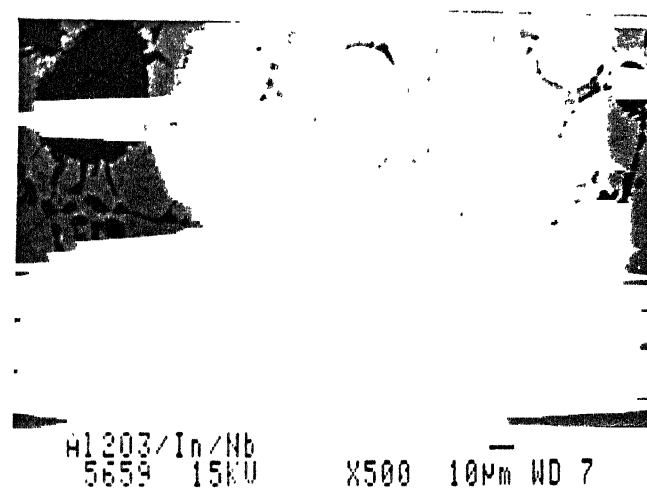


Figure 4.17:  $\alpha_2$  (Ag) phase on the filler area as bright region.

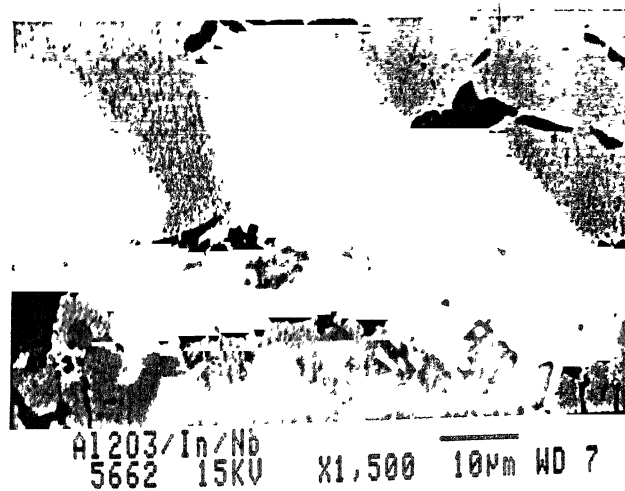


Figure 4.18: The layer of TiCu and  $Ti_2Cu$  compounds at higher magnification.

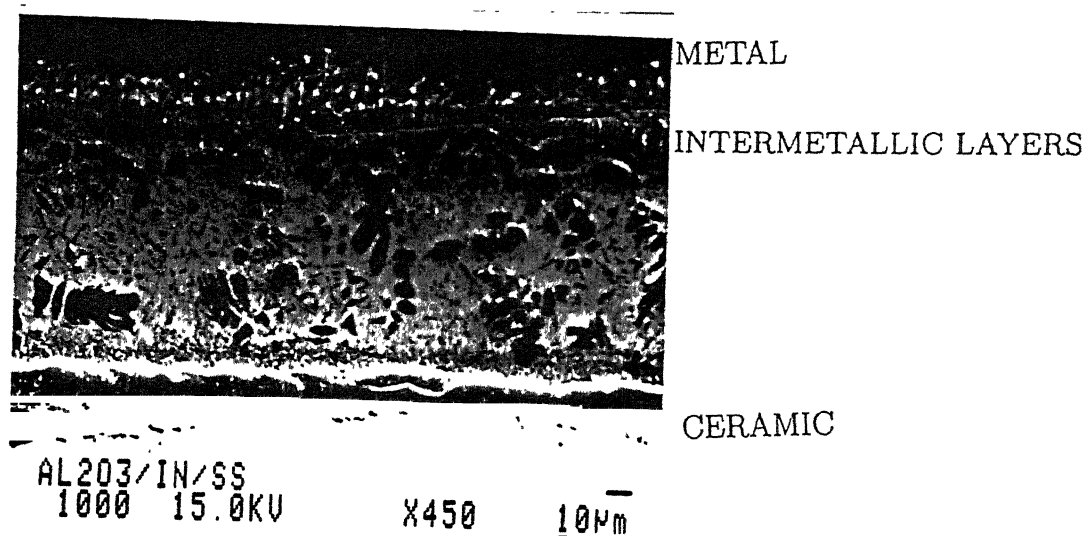


Figure 4.19: All the interfaces and layers of intermetallic compound are observed into the join area.

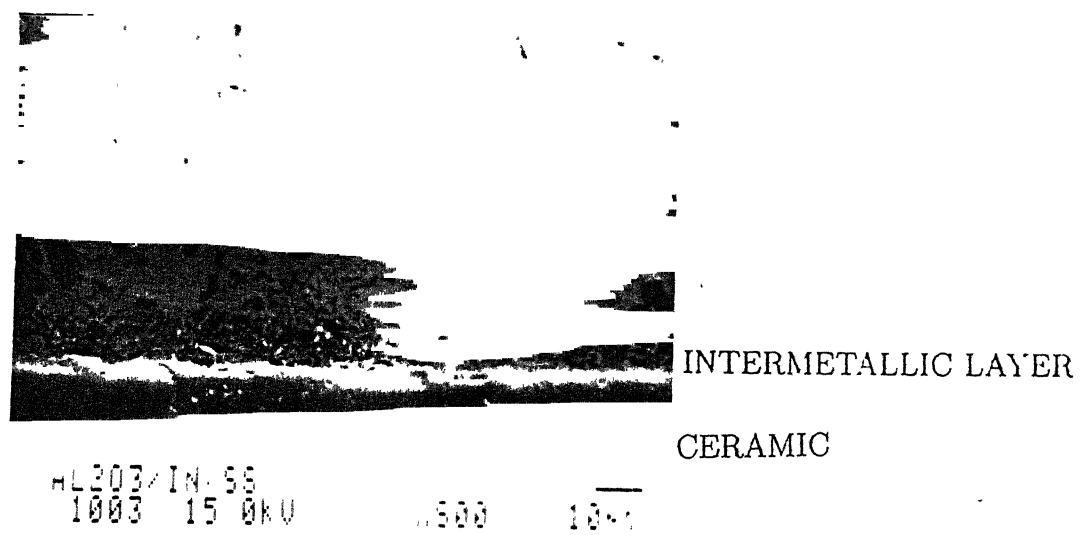


Figure 4.20: Layer of  $Ti_3Al$  compound at the Ti/alumina interface and Bright layer of AlCu phase at the Ti/filler metal interface.

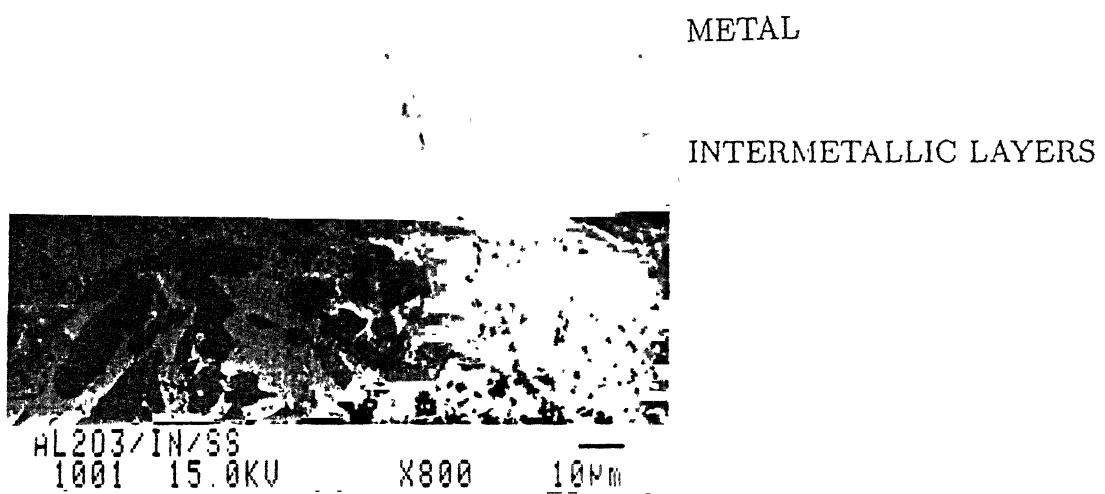


Figure 4.21: TiFe compound at the stainless steel/filler metal interface and some unknown ternary compounds are also observed next to this interface.

# Chapter 5

## Conclusion

---

- The microstructure of the phases as well as the intermetallic compounds formed at different positions of the diffusion couple is characterized.
- The binary phases of Ti-Cu, Ti-Fe and Ti-Ag systems were observed in the joints with both Ag-28Cu and Ag-27Cu-10In filler metals.
- All the phases of Ti-Cu system, such as  $TiCu$ ,  $Ti_2Cu$ ,  $Ti_2Cu_3$ ,  $Ti_3Cu_4$  and  $TiCu_4$  were observed at the Ti/filler metal interface as well as in the immediate vicinity of it.
- The binary phases from Ti-Al system such as  $Ti_3Al$  and  $TiAl_3$  were observed at the  $Ti/Al_2O_3$  interface.
- As a large number of elements are present in the ceramic to stainless steel(Fe-18Cr-8Ni) joint, large number of intermetallic layer were observed in this system.
- The unreacted filler metal Ag-28Cu as well as Ag-27Cu-10In shows only Ag-rich( $\alpha$ ) and Cu-rich( $\beta$ ) solid solution as a rod-like eutectic structure.
- Some unknown ternary phases from the Fe-Cu-Ti, Ag-Cu-Ti, Ag-Al-Cu Al-Cu-Ti, and Al-Fe-Ti systems were observed.
- An unknown binary phase from the Ag-Nb system has also been observed next to the Nb/filler metal interface.
- In the case of Niobium to alumina ceramic brazed specimen, the diffusion of Nb was limited

# References

- [1] M.Schwartz, "*Brazing : For the engineering technologist*", Chapman and Hall,1995.
- [2] Giles Hampston and David M. jacobson, "*principles of soldering and brazing*", ASM International(The Materials information society), 1993.
- [3] "*Brazing hand book*",American Welding Society, Fourth Edition, 1991.
- [4] H.Mizuhara and T. Oyama, "*ceramic/metal seals*", Reprinted from ASM hand book, Vol-4; Ceramics and Glasses, 1993.
- [5] Byeong-Joo Lee, "*prediction of Ti/Al<sub>2</sub>O<sub>3</sub> interface reaction products by diffusion simulation*", Acta mater, Vol 45, No 10, 1997, pp. 3993-3999
- [6] G.H.M Gubbels, L.S.K Heikinheimo and J.T.Klomp, "*A comparison between Titanium-Alumina Diffusion bonding and Titanium active brazing*", Z. Metallkd. 85 No. 12, 1994, pp. 828-832
- [7] M.G.Nicholas, T.M.Valentine and M.J.Waite, "*The wetting of alumina by copper alloyed with titanium and other elements*", J. Mater Sc, 15, 1980, pp. 2197-2206
- [8] E.F.BRUSH,Jr., and C.M.Adams,Jr., "*Vapor coated surfaces for brazing ceramics*.", Welding Journal, 1968, pp. 106s-114s.
- [9] M.E.Twintymen, "*High temperature metallizing: part 1 The mechanism of glass migration in the production of metal-ceramic seals*", J. Mater. Sc, 10, 1975, pp. 765-776.

[10] M.E.Twentymen, "High temperature metallizing: part 2 The effect of experimental variables on the structure of seals to debased aluminas", J.Mater.Sc, 10, 1975 pp. 777-790.

[11] M.E.Twentymen, "High temperature metallizing, pert 3: The use of metallizing paints containing glass or other inorganic bonding agents, J.Mater.Sc, 10, 1975, pp. 791-798.

[12] A.J.Moorhead and H.Keating, "Direct brazing of ceramics for advanced heavy duty diesels", Welding journal, Vol. 65, No 10, 1986, pp. 17-31.

[13] J.T.Klomp, "Interfacial reactions between metals and oxides during sealing, Am.Ceram.Soc.Bull., Vol. 59, No 8, 1980, pp. 794-802.

[14] H.Mizuhara and K.Mally, "Ceramic to metal joining with Active brazing metal", Welding Journal, Vol. 64, No 10, 1985, pp. 43-51.

[15] H.Mizuhara and E.Huebel, "Joining of ceramic to metal with ductile filler metal", Welding Journal, Vol. 65, No 10, 1986, pp. 43-51.

[16] M.Veki and M.Maka , "Wetability of some metals against Zirconia ceramics", J.Mater.Sci Lett., Vol. 5, No 12 , 1986, pp. 1261-1265.

[17] M.Nicholas and R.P.D.Forgan , "The adhesion of metal/alumina interfaces", J.Mater.Sc, Vol. 3, 1968, pp. 9-14.

[18] C.S.Kanetkar and A.S.Kanetkar , "The wetting characteristics and surface tension of some Ni based alloys on Yttria, Hafnia, Alumina and Zirconia substrate", Metall.Trans, A, Vol. 19A, 1988, pp. 1833-1839.

[19] C.Iwamoto and S.I.Tanaka, "Reactive wetting of Ag-Cu-Ti On Sic in HRTEM", Acta Mater., Vol. 46, No 7, 1998, pp. 2381-2386.

[20] J.k.Boadi and T.Yano, "Brazing of pressureless-sintered SiC using Ag-Cu-Ti alloy", J.Mater.Sc, Vol. 22, 1987, pp. 2431-2434.

[21] T.Yano and H.Suematsu, "High resolution electron microscopy of a SiC/SiC joint brazed by a Ag-Cu-Ti alloy", J.Mater.Sc, Vol. 23, 1988, pp. 3362-3366.

[22] H.K.Lee and J.Y.Lee, "Decomposition and interfacial reaction in brazing of SiC by copper-based active alloys", J.Mater.Sc, Vol. 11, 1992, pp. 550-552.

[23] J.L.Murry, Binary alloy Phase diagrams, ASM Int., Materials Park, Ohio, 1989, Vol. 2, pp. 1117-1118.

[24] T.B.Massalaski et al, Eds., Binary alloy Phase Diagrams, ASM Int, Materials Park, Ohio, 1989.

[25] J.L.Murry, Binary alloy Phase Diagrams, ASM Int., Materials Park, Ohio, 1989, Vol. 1, pp. 970-972.

[26] Ortrud Kubaschewski, Ternary alloys(A comprehensive compendium of evaluated constitutional data and phase diagrams), (Edited by G.Petzow and G.Effenberg), VCH Publishers, Newyork(USA), 1993, Vol. 2, pp. 55-59.

[27] Gautam Ghosh, Ternary alloys(A comprehensive compendium of evaluated constitutional data and phase diagrams), (Edited by G.Petzow and G.Effenberg), VCH Publishers, Newyork(USA), 1993, Vol. 5, pp. 456-469.

[28] B.C.Giessen and D. Szymanski, J.appl.Crytallgr, Vol. 4, 1971, pp. 257-259.

[29] J.Y.Brun, Z.Metallkd, Vol. 74, No 8, 1983, pp. 525-529.

[30] R.Ray, Scr. Metall., Vol. 2, 1968, pp. 357-359.

[31] Ortrud Kubaschewski, Ternary alloys(A comprehensive compendium of evaluated constitutional data and phase diagrams), (Edited by G.Petzow and G.Effenberg), VCH Publishers, Newyork(USA), 1993, Vol. 1, pp. 574-583.